Report 2131

TAYLOR MODEL BASIN
WASHINGTON, D.C.

DEPARTMENT OF THE NAVY

[redacted]

HYDROMECHANICS

AERODYNAMICS

STRUCTURAL MECHANICS

APPLIED MATHEMATICS

ACOUSTICS AND VIBRATION

SOME THEORETICAL AND EXPERIMENTAL RESULTS ON PRESSURE INTERACTION OF HYDROFOIL BOAT COMPONENTS

by

Wilburn L. Moore

HYDROMECHANICS LABORATORY

RESEARCH AND DEVELOPMENT REPORT

November 1965 Report 2131

PRNC-TMB-648 (Rev. 12-64)

SOME THEORETICAL AND EXPERIMENTAL RESULTS ON PRESSURE INTERACTION OF HYDROFOIL BOAT COMPONENTS

by

Wilburn L. Moore

November 1965

Report No. 2131
SS-600-000
Task 1703

TABLE OF CONTENTS

Page

LIST OF FIGURES

Page

Page

LIST OF TABLES

ABSTRACT

The Douglas Neumann program for non-lifting three-dimensional fluid flow is used to calculate the potential flow pressure distribution for some hydrofoil boat components in various combinations. The calculated results are compared with pressure measurements on crossed non-lifting foils, and on a lifting foil of large span in conjunction with a pod. The calculated results were corrected for lift in the latter case. These comparisons indicate that the Douglas program can be usefully applied to hydrofoil-boat problems.

Pressure calculations are presented for non-lifting strut-foil, pod-foil, and strut-pod-foil configurations. These results show that the effect of a strut on the pressure distribution of a pod-foil is appreciable, and that a pod can be used to increase the cavitation-inception speed of a strut-foil.

A discussion of how to select input points for the Douglas program for intersecting bodies is also presented.

ADMINISTRATIVE INFORMATION

This work was undertaken under Bureau of Ships Subproject SS-600-000, Task 1703.

INTRODUCTION

In order to design a subcavitating hydrofoil system without going to the time and expense of extensive experiments, it is necessary to be able to calculate the pressure distribution on a hydrofoil-strut-pod configuration. The critical (minimum) pressure calculated can then be used to predict the cavitation-inception speed of the configuration. There are many uncertainties in this last step[1] making it difficult to rely on a prediction of cavitation-inception speed, especially in a seaway, but the value of the pressure distribution to determine the relative merits of designs is unquestioned.

The general problem attacked here is: calculation of the pressure distribution on an arbitrary lifting body, excluding effects of the free surface.

The Douglas Aircraft Company has conducted studies of various parts of this problem. The most notable result of their work is a computer program to calculate the potential flow pressure distribution about a non-lifting (but otherwise arbitrary) three-dimensional shape.[2] They also have developed a program to calculate the pressure distribution about lifting two-dimensional shapes.[3]

It is the purpose of this report to show that by a proper correction method, the Douglas program for three-dimensional shapes can be used to calculate the pressure distribution about an arbitrary lifting hydrofoil-strut-pod configuration. Cavitation-inception speed may then, for given design requirements, be maximized.

---

[1]References are listed on page 19.

In addition, comparisons are presented to show the effect of a strut on the pressure distribution of a pod-foil configuration, and the effect of a pod on the pressure distribution of a strut-foil.

To facilitate use of the approach suggested here, an appendix is included describing how to choose the computer input points for a complicated configuration.

THE DOUGLAS NEUMANN PROGRAM FOR THREE-DIMENSIONAL FLOW

When using the Douglas program, one inputs a set of x, y, z coordinates defining the configuration whose pressure distribution is to be computed. The program then forms quadrilateral elements from these points, calculates the induced velocities due to unit singularities placed on each quadrilateral, and adjusts the strengths of the singularities so that the induced velocities from all the quadrilaterals when added to the free-stream velocity, give a normal velocity of zero at each element. The total velocity at each element is then calculated by adding the total induced velocity to the free-stream velocity.

When incompressible inviscid flow is being considered, the pressure coefficient $(\frac{P - P_\infty}{1/2 \rho V_\infty^2})$ may be calculated from $C_p = 1 - (\frac{V}{V_\infty})^2$, where V is the local velocity and V_∞ is the free-stream velocity. Any body, the non-redundant part of which can be defined by approximately 600 quadrilateral elements or fewer, can be handled by the program. A pressure calculation for complicated bodies such as those discussed in this report requires from one to four hours of IBM 7090 computing time. A detailed description of this pressure-calculation method can be found in Reference 2. Additional discussion on its use may be found in References 4 and 5.

The Douglas Neumann Program can also be used to calculate, to a first order approximation, the compressible flow about three-dimensional bodies. (See Appendix A.)

CROSSED FOILS

Hess and Smith[2] presented many experimental comparisons to demonstrate the accuracy of their pressure calculations. However, no comparison was given for an area very close to the intersection between two bodies. Since this is a critical area, a test was made at the David Taylor Model Basin to determine whether the Douglas Neumann Program could predict these pressures adequately. The configuration chosen consisted of two uncambered large-aspect-ratio foils of equal chord and unequal thickness intersecting at right angles. The configuration is described in detail in Appendix B.

This crossed-foil model was built and tested for pressure distribution in the DTMB 8-ft x 10-ft Subsonic Wind Tunnel with each foil fully spanning the tunnel. The tests were run at a free-stream Mach number of 0.221; the pressure coefficient was based on local tunnel static pressure; the results were corrected for blockage effects; and no artificial turbulence stimulators were used.

Since the configuration had two planes of symmetry, pressure measurements were necessary only in one quadrant of the configuration. However, to check for symmetry and to compensate for any imperfect alignment, some orifices were located on each side of each foil leg. Some of the pressure results were corrected slightly for these effects.

The pressure distribution for this configuration was calculated by the Douglas Neumann Program using the Goethert transformation to compensate for compressibility effects. (See Appendix A.) Note that these compressibility corrections are not part of any hydrofoil problem but are a consequence of the decision to run these tests in air.

Comparisons of the calculated results with the experimental results are presented in Figures 1 and 2. (The calculated pressure values are slightly different from those previously published by Faulkner[6] since the calculated values used by Douglas were not corrected for compressibility.) At the intersection the results agree quite well for about the forward 1/3 of the chord length. Aft of this region the boundary layer interference is so large that it causes large increases in the measured pressures. The aft results agree better farther out along the span where the boundary layers do not interact.

The two-dimensional pressure distribution for each of the foil shapes was calculated using the isolated two-dimensional airfoil option of Reference 3, with the Kármán-Tsien correction applied for compressibility.[7] These curves (Figures 1 and 2) show that the interference effects due to the thin foil are almost negligible at two chords distance from the intersection on the thick foil. The interference effect of the thick foil on the thin foil is slightly larger at two chords along the span.

The differences in the intersection critical pressures between the calculated and measured results correspond to a difference of 1/2 of a knot (1.3%) in cavitation-inception speed in salt water at 5-foot depth (calculated by assuming that the critical pressure is equal to the water vapor pressure).

POD-FOIL WITH LIFT

Since all hydrofoils of practical interest operate at non-zero lift, a problem of primary interest is the interference effect of pods and struts on a lifting foil. The Douglas program has been shown to be useful in predicting interference effects on non-lifting configurations, so a logical next step is an attempt to correct results of a non-lifting calculation for effects of lift. No satisfactory pressure data for interference flow in water were found, necessitating the use of aerodynamic data and a compressibility correction for the theoretical calculations.

The Goethert transformation has been shown to be a useful correction technique for compressibility (See Appendix A.) but it is not very convenient for bodies at non-zero angle of attack. For this reason, the most useful experimental data were from Reference 9, which used a model at zero angle of attack, with lift provided by wing camber. This test configuration consisted of a modified NACA fuselage form 111 with an unswept, untapered, large-aspect-ratio, modified NACA 65-210 wing whose chord line coincided with the axis of the fuselage. The details of the configuration are presented in Appendix C. Since this work is directed to hydrofoil boat application, the wing will be referred to as the foil and the fuselage will be called the pod.

In order to have the configuration in a form that the Douglas three-dimensional program could handle (i.e., no lift), the non-lifting foil from which 65-210 was derived, the 65-010, was used in conjunction with the fuselage form 111 as the input shape for the Douglas non-lifting three-dimensional program. The Goethert transformation was used to correct for compressibility. (See Appendix A.)

To correct for lift the pressure calculations on the foil part of the pod-foil, two-dimensional pressure distributions were calculated[3] for the 65-010 at a lift coefficient (C_L) of zero, and for the 65-210 at $C_L = 0.17$ which is the two-dimensional C_L for zero incidence.[10] Each of these pressure distributions was then corrected for compressibility by the Kármán-Tsien method.[7] The difference between these two pressure distributions was then used to correct the non-lifting pressure calculations on the foil.

The same lift correction was used all along the span since, in the tests, the configuration spanned the entire tunnel. The comparison of the theoretical and experimental results will show whether this approach was valid. Obviously, for the usual hydrofoil design case, a method would have to be used to calculate the distribution of lift along the span.

The results of the theoretical and experimental comparison on the wing are presented in Figures 3 and 4. Figure 3 gives the results essentially right at the intersection of the pod and foil. (See Figure 16, discussed in Appendix C.) The theoretical results agree quite well with the measurements on the suction side (the critical area for cavitation), and are appreciably in error on the pressure side. It may be noted that the problem of boundary layer interaction is not nearly so apparent here as it was on the crossed foil. This is due in part to the fact that the pressure orifices were not located right at the intersection in the pod-foil but rather were along a line parallel to the free-stream direction. Also the intersection itself is less curved in the pod-foil than in the crossed-foil.

The pressure comparison at approximately half a foil chord away from the pod intersection, (See Figure 16 discussed in Appendix C.) where most of the interference effects have died out, is presented in Figure 4. Here the agreement between the experimental and calculated results is somewhat better than it was nearer the intersection. The cavitation-inception speed difference between the calculated critical pressure and the measured one is about 1/3 knot here, (0.7%) whereas it is 1 knot (2.5%) at the intersection.

A similar method was used to correct the pod pressures for the effect of the foil lift. Using the isolated airfoil option of the Douglas Neumann two-dimensional cascade program,[3] which can also calculate pressures at points not on the body surface, the pressures were calculated at points the same distance above the two-dimensional foil as the points on the pod are above the actual foil. This was done for both the 65-010 shape and the 65-210 shape. These pressures were each corrected for compressibility by the Kármán-Tsien method.[7] The pressure at each point induced by the 65-010 foil was then subtracted from that induced by the 65-210 foil. This difference was then multiplied by z/R where z is the distance the point on the pod is above the foil and R is the three-dimensional distance from the point on the pod to the nearest point on the foil. These values were used to correct the non-lifting pressures on the pod for effects of lift on the foil. The results of these calculations are presented in Figure 5 along with the measured pressures. As could be expected, since the lift correction technique is less justified, the results on the pod do not agree as well as those on the wing. The calculated critical pressure predicted a cavitation speed about 2 knots (4.2%) too high on the pod. The results near 25 percent of the pod length, which is where the leading edge of the foil intersects the pod, are appreciably in error. This is partly due to the nature of the quadrilaterals chosen to define the configuration in this area. For this reason the pressures in the area near 25 percent of the length are unreliable.

STRUT-POD-FOIL, POD-FOIL, AND STRUT-FOIL

In analyzing the pressure distribution on the foil of a strut-pod-foil configuration, the presence of a thin strut is often ignored to simplify the analysis.[11] Similarly, it is occasionally asserted that the installation of an otherwise unneeded pod at the intersection of a strut and foil may increase the cavitation-inception speed of the configuration.[12]

To test the validity of these hypotheses, a series of calculations were made using the Douglas Neumann Program. The basic components used were: a foil with semi-span = 1000 (dimensionless), chord = 50, and thickness = 5; a strut of the same dimensions except that 1000 was the full span; a pod of length = 100, and diameter = 20. Each of these components was a derivation of the DTMB Series 58, Model 4162 shape.[17]

A pressure calculation was run on the strut-foil configuration (an inverse T shape) shown in Figure 17 (discussed in Appendix D). The pressure distribution on the foil part of this configuration is presented in Figure 6.

A pressure calculation was run on the pod-foil configuration shown in Figure 18 (discussed in Appendix D). The pressure distribution on the upper foil surface is presented in Figure 7, and that of the pod in Figure 8.

A pressure calculation was run on the strut-pod-foil configuration shown in Figure 19 (discussed in Appendix D). The pressure distribution for the foil upper surface is presented in Figure 9, for the pod upper surface in Figure 10, for the pod lower surface in Figure 11, and for the pod nose and tail in Figure 12. A detailed description of the strut-pod-foil configuration is presented in Appendix D, and a description of the procedure for choosing the input points for the computer program is presented in Appendix E.

Figure 13 shows the effect of the 10 percent thick strut on the pressure distribution of a pod-foil. It can be seen that, far from being negligible, the strut causes a large decrease in pressure at the intersection. At a depth of 5 feet in salt water, this pressure decrease would decrease the cavitation-inception speed of the configuration by 5 knots (8.5%).

Heretofore, the strut in a strut-pod-foil configuration was dealt with rather lightly from a hydrodynamic point of view since the critical pressure clearly would not occur there. These results indicate that the strut should be made as thin as possible, consistent with structural requirements, in order that the detrimental effect on the foil pressure may be minimized.

The effect of a pod on the pressure distribution of a strut-foil can be seen in Figure 14. (The configuration is sketched in Figure 19, discussed in Appendix D.) Figure 14 shows that the installation of this pod increases slightly the cavitation-inception speed of the configuration. This is true despite the large thickness of the pod (L/D = 5). However, this large pod thickness is beneficial in one way—it separates the foil from the strut a larger distance than would a finer pod of the same length.

CONCLUSIONS

1. The Douglas Neumann Program can predict accurately the pressure at the intersection in a complex configuration for about one-third the length of the intersection, at which point the boundary layer interaction begins to dominate the flow.

2. When finite wing effects are not present, a simple lift correction to the Douglas non-lifting three-dimensional program applied to a pod-foil

configuration gives very good correlation with measured pressures on the suction side of the foil, but does not give good correlation on the pressure side.

3. The addition of an otherwise unneeded pod at the intersection of a strut and foil can be utilized to delay the onset of cavitation.

4. A strut has an appreciable adverse effect on the pressure distribution of a pod-foil.

RECOMMENDATIONS

1. Struts on a strut-pod-foil configuration should be designed for maximum cavitation-inception speed so that the adverse effect of the strut on the foil pressure distribution will be minimized.

2. Further calculations should be made to determine appropriate lengths and fineness ratios for pods to be used for raising the cavitation-inception speeds of strut-foil configurations.

3. A comparison should be made between measured pressures on a strut-pod-foil configuration with a finite lifting wing, and a pressure calculation by the present method with a suitable technique for predicting the spanwise distribution of lift.

ACKNOWLEDGMENTS

The author acknowledges the assistance of personnel of the Subsonic Division of the TMB Aerodynamics Laboratory, especially Messrs. Elmer T.

Burgan and John T. Matthews, who conducted the crossed foil tests; Mr. George H. Smith of the Applied Mathematics Laboratory; and Mr. Douglas R. Harry of the Hydromechanics Laboratory, who prepared the figures.

APPENDIX A - PRESSURE DISTRIBUTION FOR COMPRESSIBLE FLOW

The Douglas Neumann Program can be used to calculate, to a first order approximation, the compressible flow about three-dimensional bodies. This can be done by using the Goethert transformation technique which has been shown to be accurate, especially for low Mach numbers. (See Sears[13] and references cited.) This method involves "stretching" the configuration in the streamwise direction by dividing its streamwise coordinates by $\sqrt{1 - M_\infty^2}$ where M_∞ is the free-stream Mach number. The potential flow velocities are then calculated for this stretched body using the Douglas program. The induced velocity components for compressible flow are then $U = U'/(1 - M_\infty^2)$, $V = V'/\sqrt{1 - M_\infty^2}$, $W = W'/\sqrt{1 - M_\infty^2}$, where the primes denote induced velocities calculated about the stretched body.[14] The total velocity is calculated by adding the free-stream velocity to the induced velocities. The pressure coefficient for compressible flow is not simply $1 - (V/V_\infty)^2$ since the density is no longer constant. If one assumes isentropic flow the pressure coefficient can be calculated by[15] $C_p = \frac{2}{\gamma M_\infty^2}\left\{\left[1 + \frac{\gamma-1}{2} M_\infty^2 \left(1 - \frac{V^2}{V_\infty^2}\right)\right]^{\frac{\gamma}{\gamma-1}} - 1\right\}$, where γ is the ratio of specific heat at constant pressure to specific heat at constant volume, which is 1.4 for air in the temperature range of present interest.[16]

This Goethert transformation is built into some versions of the Douglas Neumann three-dimensional program. A separate program (DTMB Open Shop No. XM14) was written for this correction at the David Taylor Model Basin.

APPENDIX B - CROSSED FOIL CONFIGURATION

The basic shape used for this configuration was the DTMB Series 58 Model 4162, whose meridional (or two-dimensional, as the case may be) shape is defined by $y^2 = a_1x + a_2x^2 + a_3x^3 + a_4x^4 + a_5x^5 + a_6x^6$, where x is the dimensionless axial offset based on body length (or chord length) and y is the dimensionless transverse offset based on maximum diameter, and

a_1 = +1.0000000	a_4 = +20.564584
a_2 = +0.44469380	a_5 = -20.948726
a_3 = -8.9197388	a_6 = 7.8591877.

The "a" values are slightly different from those values reported by Gertler[17] for the same shape. So many offsets of this shape were needed for the present work that the "a" values were recalculated to higher precision, and used to generate a larger number of axial offsets. Near the trailing edge of the shape, the generating function involves square roots of small differences of large numbers, so every bit of precision helps. Even with these new coefficients, there is an error of the order of 0.001L in the transverse offsets near the tail.

In the theoretical model, the basic dimensions were: horizontal thick foil - length = 100 (dimensionless), thickness = 20, semi-span = 1000. Vertical thin foil - length = 100, thickness = 10, semi-span = 1000. Since the configuration has two planes of symmetry, it was only necessary to input one quadrant.

A proper balance of computer time and calculation accuracy led to the choice of coordinates listed in Table 1, which were input at the following spanwise locations: at the intersection, 0.1 along the span away from the intersection, 11, 20, 40, 60, 140, 260, 1000. (The numbers refer to distance to the plane of symmetry, except for the first two values which refer to the intersection.)

In the wind tunnel, the model was built with each foil having a 1-ft chord, the 20 percent thick horizontal foil spanning the 10-ft width and the 10-percent thick vertical foil spanning the 8-ft height of the tunnel. There were no fillets at the intersections. A picture of the configuration is presented in Figure 15.

APPENDIX C - NACA POD-FOIL CONFIGURATION

This configuration consisted of a modified NACA fuselage form 111 and an unswept, untapered, large-aspect-ratio modified NACA 65-210 wing whose chord coincided with the axis of the fuselage. The modification of the wing (or foil) for the wind tunnel tests consisted of removing 2.22 percent of the chord length of the wing from the trailing edge. This alleviated the structural problem created by the extreme thinness of this part of the model wing. This modification was not made to the configuration used for the theoretical pressure distribution because the discontinuity would make the calculations more difficult, and no more reliable. (Where dimensionless wing lengths are used they are based on the unmodified length.)

The basic pod shape was a variation of the NACA fuselage form 111 whose shape was modified for the purposes of the NACA tests (See Reference 9.) to improve the fairing in the area near 20 percent of the length. Its fineness ratio was 6 and its length was approximately 2.6 wing chords. The wing leading edge was at 25 percent of the pod length, and the trailing edge at 63.46 percent. The configuration for which the calculations were made corresponds to position C_3 of Reference 9, with no filleting of the intersection.

The offsets for the pod are presented in Table 2, those for the foil in Table 3. The spanwise locations of the pressure orifices are shown in Figure 16. The theoretical results are presented for the same locations.

Further details on the configuration are available in Reference 9.

APPENDIX D - STRUT-POD-FOIL CONFIGURATION

The basic function generating each of the shapes in this configuration is the same as that which was used for the crossed-foil configuration. (See Appendix B.) The pod length was 100 (dimensionless), with maximum diameter equal to 20. The offsets used are given in Table 4. The foil chord was 50 with a maximum thickness of 5. The leading edge of the foil intersected the pod at 25 percent of the pod length, the trailing edge at 75 percent of the pod length.

The strut dimensions were identical with those of the foil. For both foil and strut, the span was chosen large enough (2000, 1000) that the tip effects were negligible in the region of the pod. The arrangements of the components in the strut-foil, pod-foil, and strut-pod-foil configurations are shown in Figures 17, 18, and 19.

APPENDIX E - INPUT POINT DISTRIBUTION FOR INTERSECTING SHAPES

How to choose input points in the Douglas Neumann three-dimensional program for a configuration with an intersection will be discussed in some detail since this is an application that is likely to recur often. The strut-pod-foil configuration will be used as an example.

The x-axis is the axis of the pod with the x = 0 plane at the pod nose. The y-axis runs along the horizontal foil span with the y = 0 plane coincident with the chord plane of the vertical strut. The z-axis runs along the span of the vertical strut with the z = 0 plane (z positive upwards) coincident with the chord plane of the horizontal foil.

The configuration has a vertical plane of symmetry permitting it to be described by offsets for only one side.

For ease of input the configuration was divided up as follows: The strut was one section, the foil was divided into an upper surface section and a lower surface section; the pod was cut up into three parts, the nose which was a section, the tail which was a section, and the middle portion which extended over that part intersected by the strut and foil (x = 25 to x = 75). The pod middle portion was further divided into an extreme lower section, a section intersecting the lower foil surface, a section intersecting the upper foil surface, a section intersecting the strut, and a section between the latter two.

These sections were chosen because of different input point density requirements in the different areas. To save computer time (or in this case, to describe the configuration within the input limits of the program), one should distribute points sparsely in geometrically smooth areas and in areas of little interest.

In the strut-pod-foil configuration, the areas of maximum interest are the foil upper surface near the pod, and the pod surface near the foil. These are also areas of abrupt change in geometry. A large number of input points are clearly needed there.

The pod near the strut is an area of some interest and also of abrupt curvature. The intersection of the lower surface of the foil with the pod is of no real interest, but is an area of abrupt geometric change. On the other hand, the strut is of minimal interest and of simple geometry, as is the lower surface of the foil.

With these considerations in mind the point spacing was made very sparse on the strut except very near the pod intersection. The lower surface of the foil was treated similarly. The pod nose and tail were of no major interest so just enough points were chosen to define the curvature smoothly enough that the pressure results in the areas of interest were not adversely affected. The lower 60-degrees of the middle portion of the pod was treated similarly.

The upper surface of the foil, being the area of main interest, required a large number of input points even at appreciable distances from the pod intersection, so that the pressure could be calculated at enough points to define the pressure distribution along the chord and span. The area, both on the foil and on the pod, near the intersection of the foil upper surface with the pod presented the greatest problem. This is an area of great interest since the critical pressure for the configuration is likely to occur there, and there is a discontinuity in geometry there, also.

Longitudinally, 21 points were considered sufficient to define the curvatur of the lines near the intersection. Points were concentrated near the forward part of the intersection where the curvature was greater.

Transversely, in addition to economy of points, there are two opposing considerations which must be weighed. On the one hand is the fact that the more densely one distributes the points in a region of abrupt change in geometry, the more precisely will the body be defined. On the other hand, the Neumann problem is only solvable for bodies with continuous values of normal derivative on the body contour.[18] It is clear that at the intersection of the foil and pod, the normal derivative is discontinuous. Practically though, the normal derivative will never be evaluated right at the intersection by the program since the derivative is evaluated at the null point,[19] rather than at the corners of an element. (The null point is usually close to the centroid of the element.) Therefore, the denser the distribution of points (transversely) near the intersection, the closer the program gets to evaluating a normal derivative at the intersection, and the more abrupt will be the change in the normal derivative. Thus the requirements as to transverse density of input points near the intersection reduce to these: dense enough to define the shape fairly well, but not dense enough to produce too drastic a variation in the normal derivative.

In a given calculation, one can tell after the calculation whether the distribution chosen was appropriate by comparing the pressure values of the points closest to the intersection on the pod and the points closest on the foil. If the points were too sparse, the values will differ noticeably; if the points were too dense, the values will differ drastically.

After much experimentation, the following distribution chosen for the upper foil-pod intersection was found to be satisfactory. The other intersections in this problem were treated less carefully since they were of less interest. At the upper foil-pod intersection the input points were distributed thusly: one line at the intersection; one line 0.2 (or 0.004 wing chords), measured circumfuentially along the surface of the pod, away from the intersection; 0.5 away from the intersection; at 30 degrees (measured from the plane of the foil chord and the pod axis); and between 0.5 away and 30 degrees a line representing the mean distance along the pod surface between 0.5 away and 30 degrees. On the foil, a line was placed at the intersection; 0.2 along the span away from the intersection; and at the following spanwise stations (measured from the vertical plane of symmetry of the configuration), 11, 20, 40, 60, 140, 260, and 1000.

All of the offsets for the strut-pod-foil are given in Table 5.

REFERENCES

1. "Handbook of Fluid Dynamics," Edited by V. L. Streeter, McGraw-Hill Book Co., Inc., New York (1961), "Mechanics of Cavitation," (Phillip Eisenberg), pp. 12-16.

2. Hess, J. L. and Smith, A. M. O., "Calculation of Non-Lifting Potential Flow about Arbitrary Three-Dimensional Bodies," Douglas Aircraft Co., Inc., Report E.S.-40622 (1962).

3. Giesing, J. P., "Extension of the Douglas Neumann Program to Problems of Lifting, Infinite Cascades," Douglas Aircraft Co., Inc., Report LB 31653 (1964).

4. Denny, S. B., "Applicability of the Douglas Computer Program to Hull Pressure Problems," David Taylor Model Basin Report 1786 (1963).

5. Faulkner, S., et al, "Comparison of Experimental Pressure Distributions with Those Calculated by the Douglas Neumann Program," Douglas Aircraft Co., Inc., Report No. LB 31831 (1964).

6. Reference 5, pp. 86, 87.

7. Dwinnell, J. H., "Principles of Aerodynamics," McGraw-Hill Book Co., Inc., New York (1949), p. 180.

8. Reference 5, pp. 79-84, 92.

9. McLellan, C. H. and Cangelosi, J. I., "Effects of Nacelle Position on Wing-Nacelle Interference," NACA T.N. 1593 (1948).

10. Abbott, I. H. and von Doenhoff, A. E., "Theory of Wing Sections," McGraw-Hill Book Co., Inc., New York (1949), p. 612.

11. Johnson, R. S., "Prediction of the Lift and Cavitation Characteristics of Hydrofoil-Strut Arrays," Paper presented at the Southern California Section, Society of Naval Architects and Marine Engineers (Mar 1964), p. 12.

12. Clement, E. P., "Research to Eliminate Cavitation on the PC(H) Hydrofoil Boat Design," David Taylor Model Basin Report C-1233 (1960), p. 7 (CONFIDENTIAL).

13. Sears, W. R., editor, "General Theory of High-Speed Aerodynamics," Princeton University Press, Princeton, N. J. (1954), p. 88.

14. Reference 13, p. 81.

15. Liepmann, H. W. and Roshko, A., "Elements of Gasdynamics," John Wiley and Sons, Inc., New York (1957), p. 55.

16. Kuethe, A. M. and Schetzer, J. D., "Foundations of Aerodynamics," Second Edition, John Wiley and Sons, Inc., New York (1959), p. 133.

17. Gertler, M., "Resistance Experiments on a Systematic Series of Streamlined Bodies of Revolution -- For Application to the Design of High-Speed Submarines," David Taylor Model Basin Report C-297 (1950), p. 56 (CONFIDENTIAL).

18. Kellogg, O. D., "Foundations of Potential Theory," Frederick Ungar Publishing Co., New York (1929), p. 311.

19. Reference 2, p. 74.

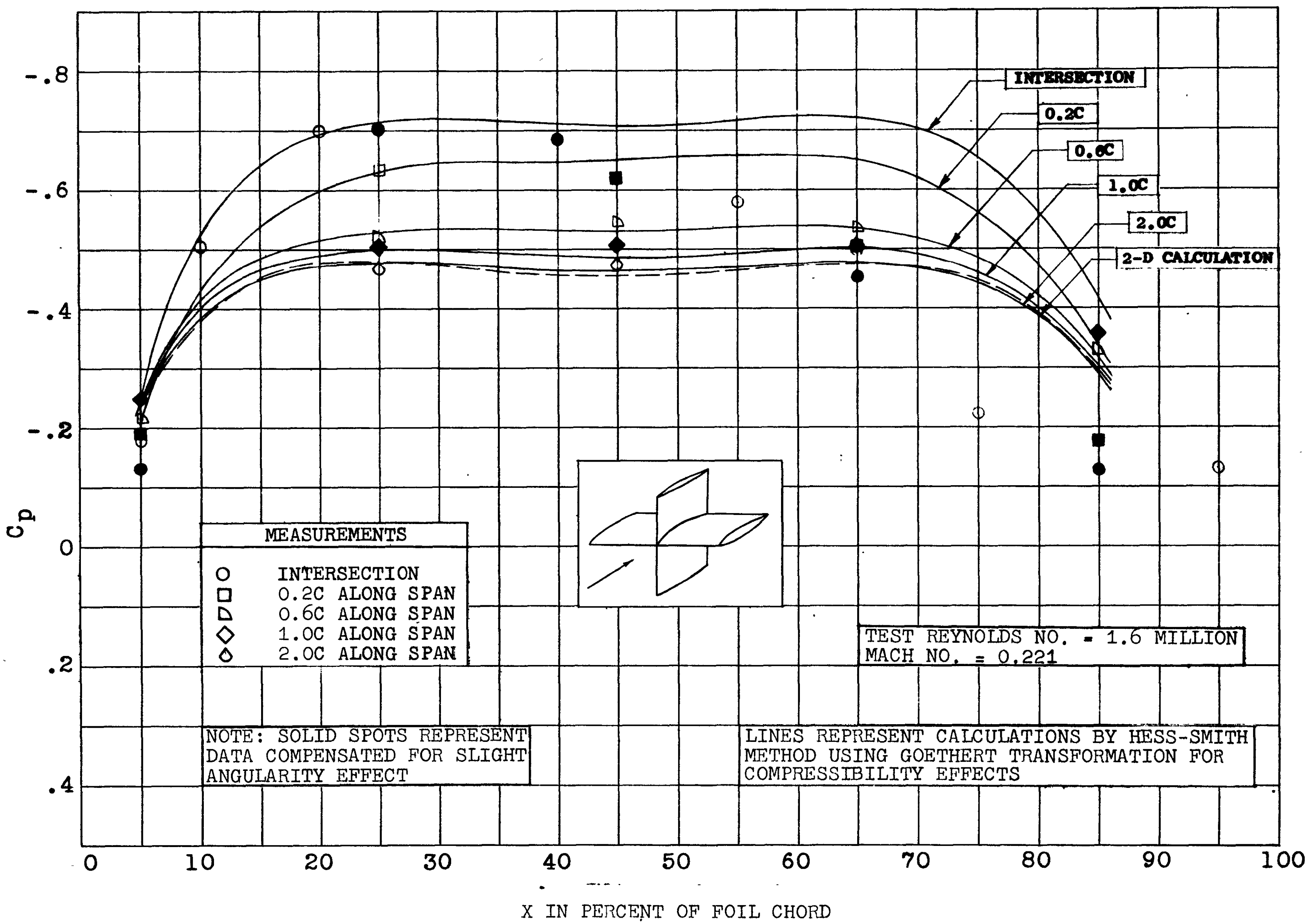

Figure 1 - Comparison of Experimental Values with Calculated Values of Pressure Coefficient for Crossed Foils of Equal Chords and Unequal Thicknesses at Zero Lift: Pressures on Thick Foil (20% Thick)

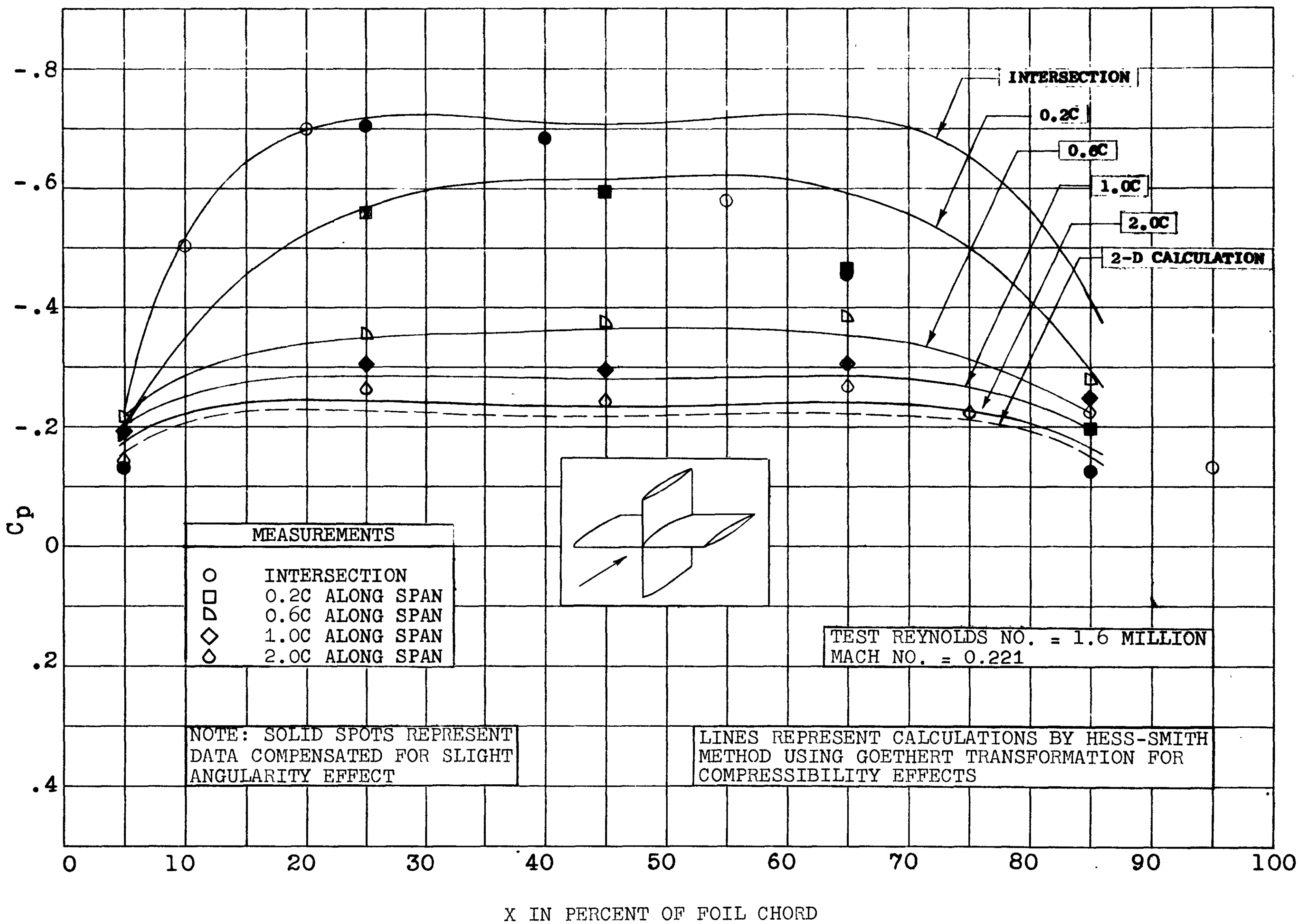

Figure 2 - Comparison of Experimental Values with Calculated Values of Pressure Coefficient for Crossed Foils of Equal Chords and Unequal Thicknesses at Zero Lift: Pressures on Thin Foil (10% Thick)

NO 4520-L 20X20 TO THE INCH

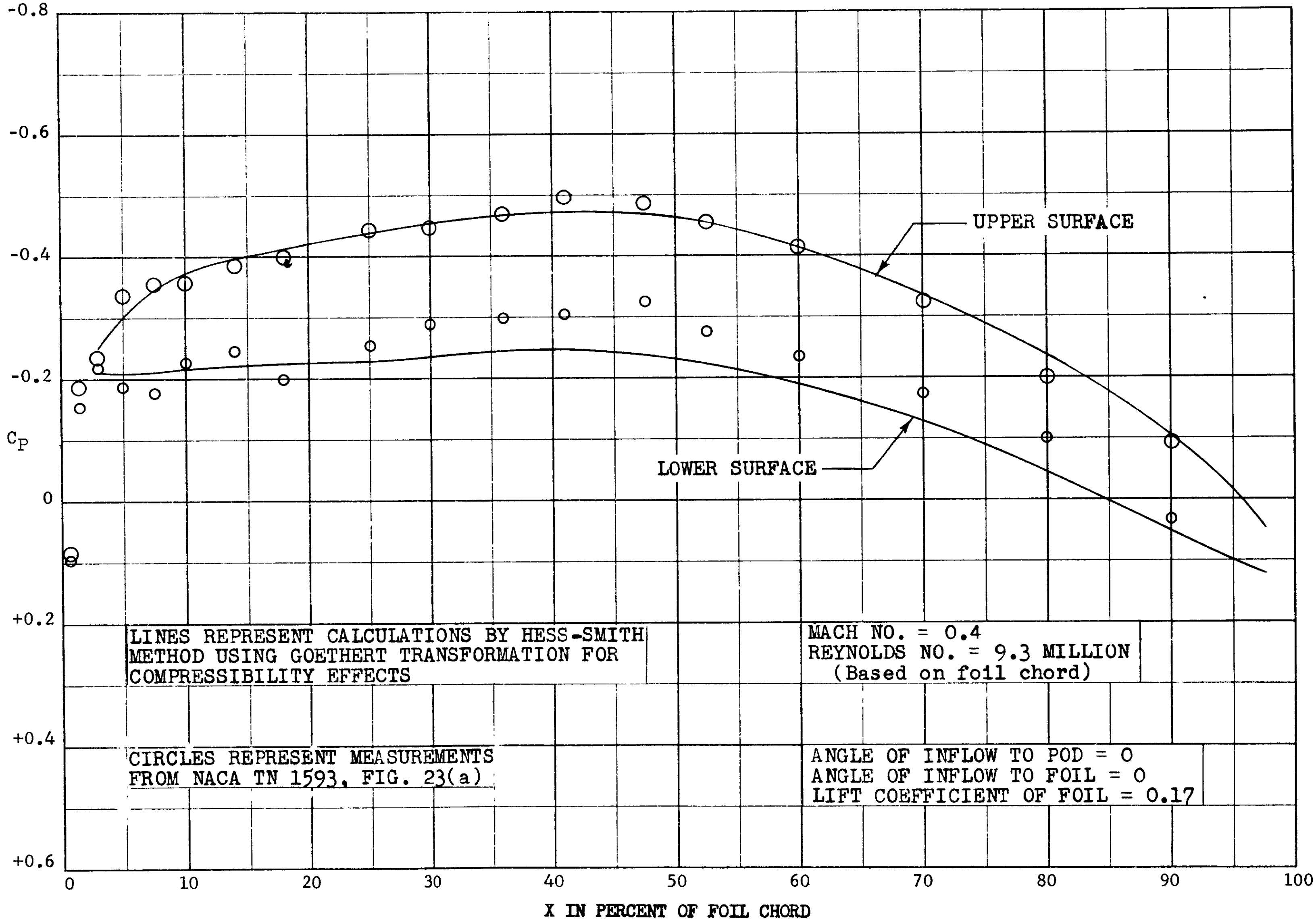

Figure 3 - Comparison of Experimental Values with Calculated Values of Pressure Coefficient for Pod-Foil Configuration with Lift: Points on Foil at Intersection

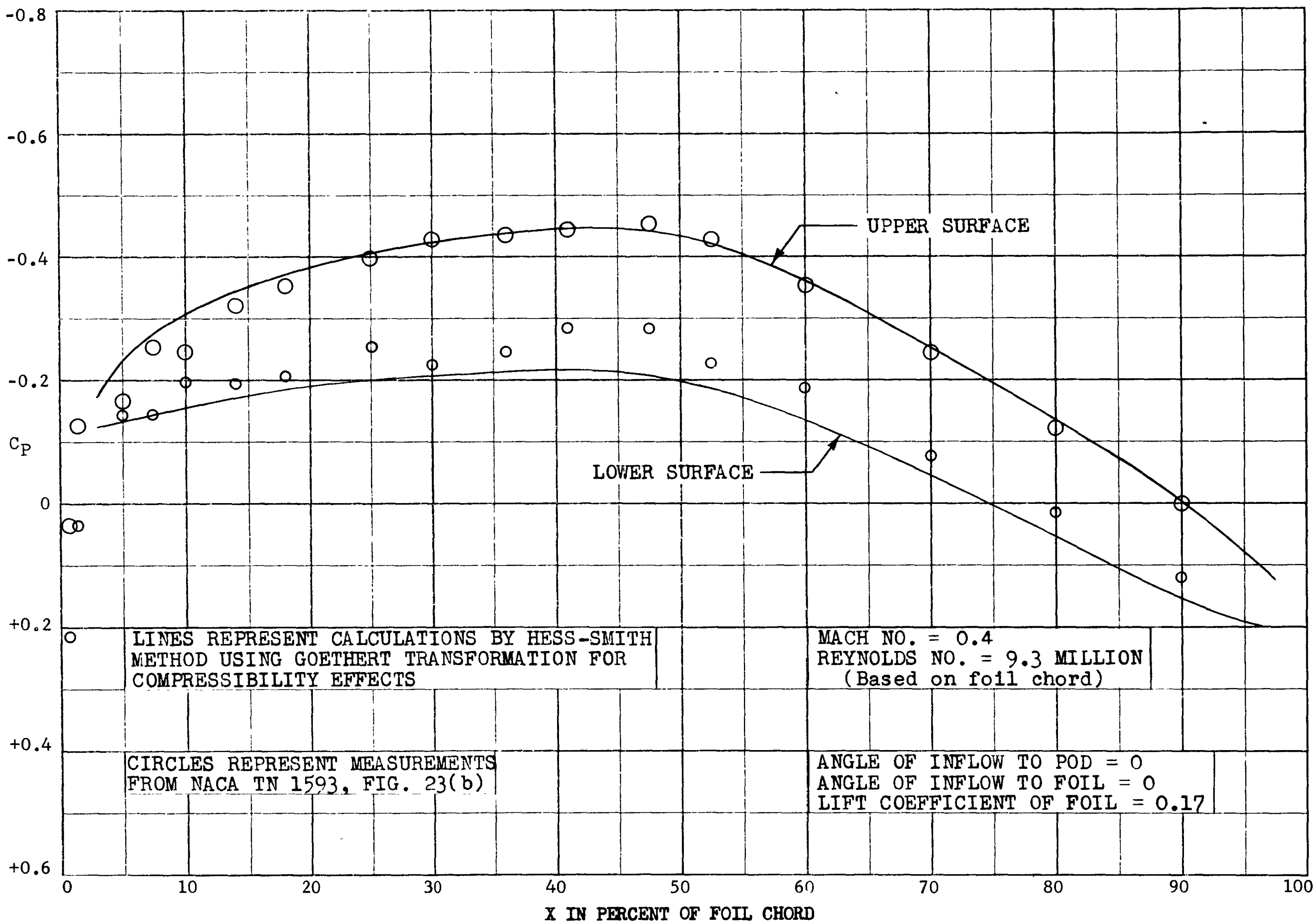

Figure 4 - Comparison of Experimental Values with Calculated Values of Pressure Coefficient for Pod-Foil Configuration with Lift: Points on Foil away from Intersection

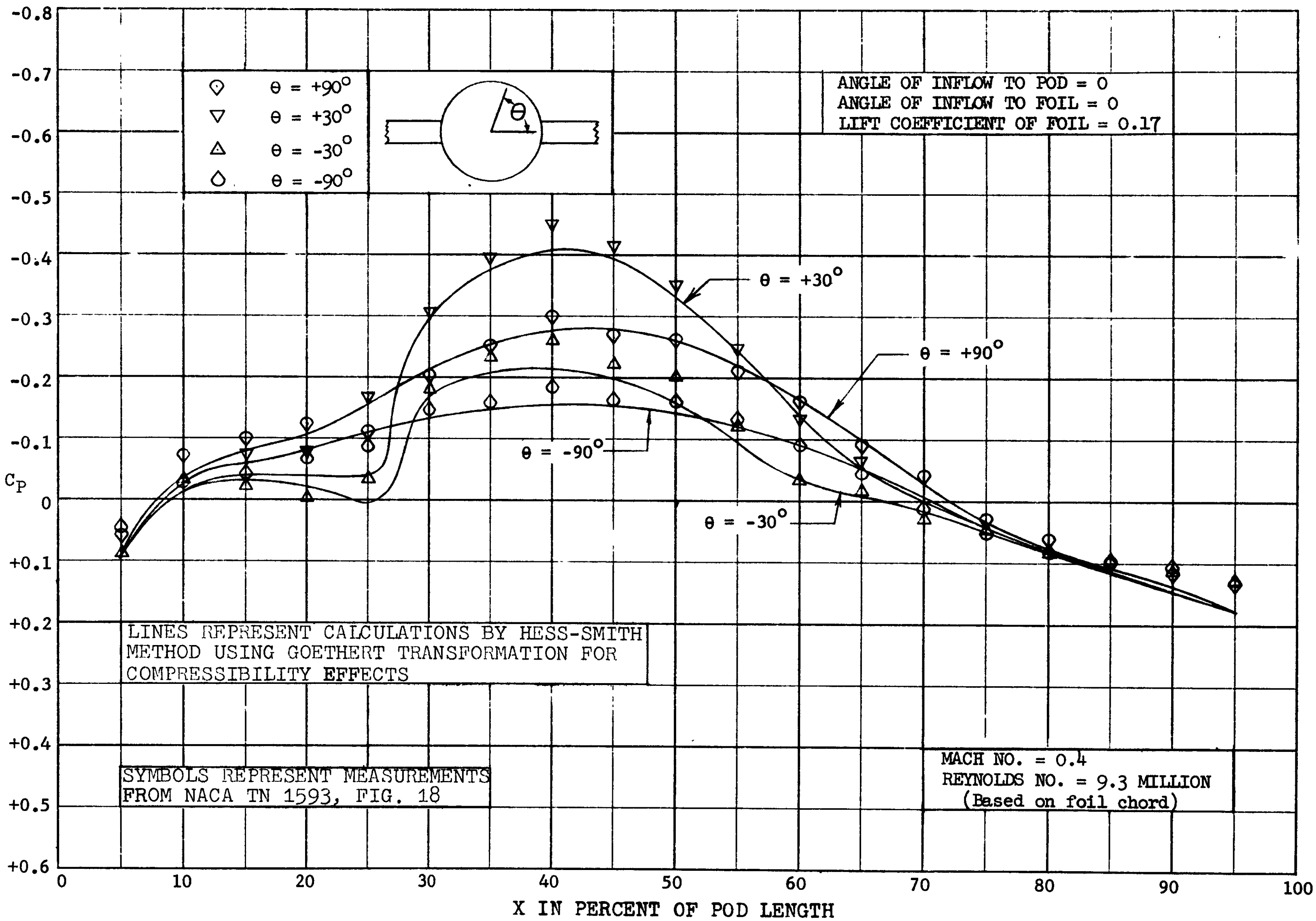

Figure 5 - Comparison of Experimental Values with Calculated Values of Pressure Coefficient for Pod-Foil Configuration with Lift: Points on Pod

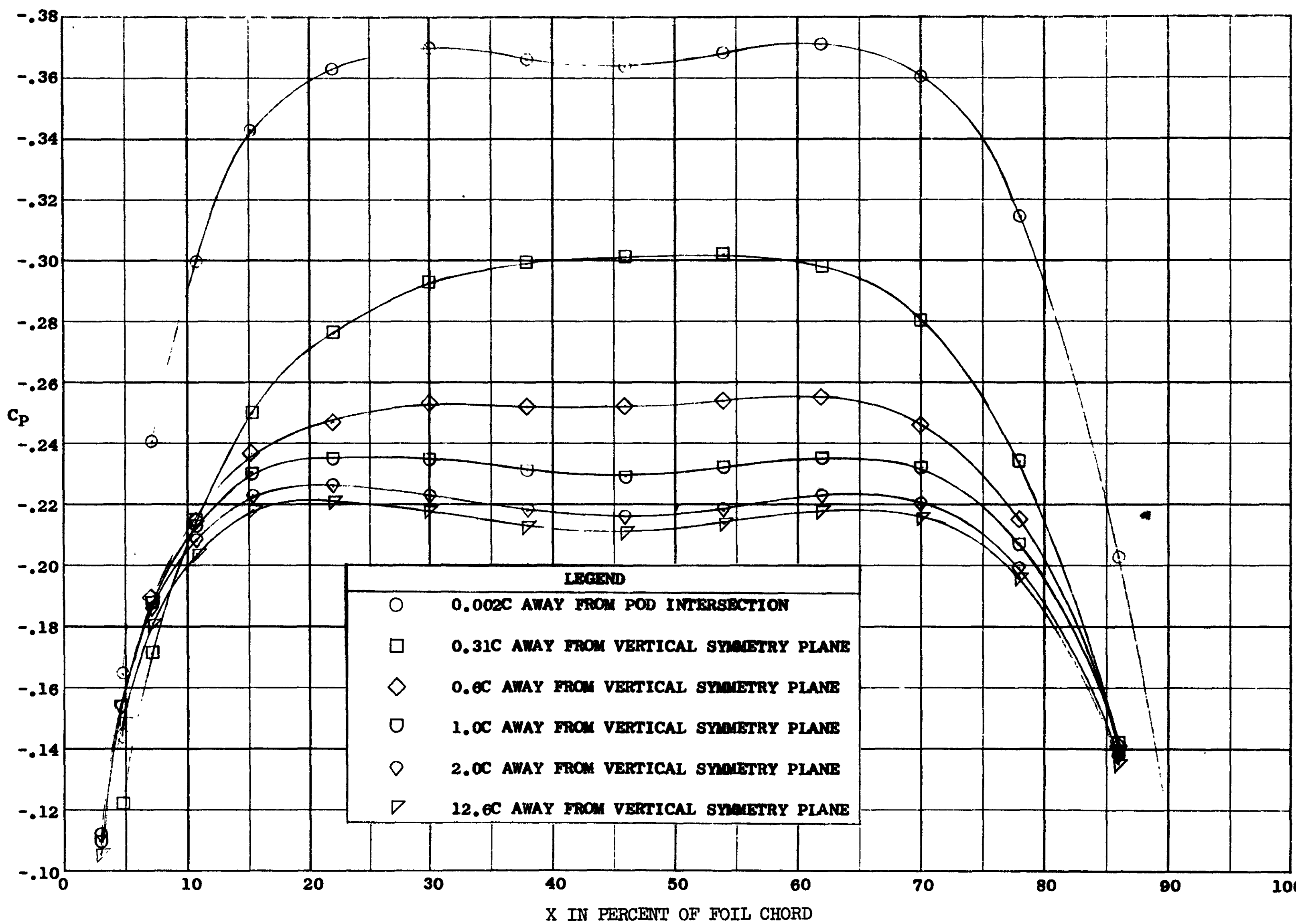

Figure 6 - Potential Flow Pressure Distribution on Foil Upper Surface of Strut-Foil Configuration at Zero Lift

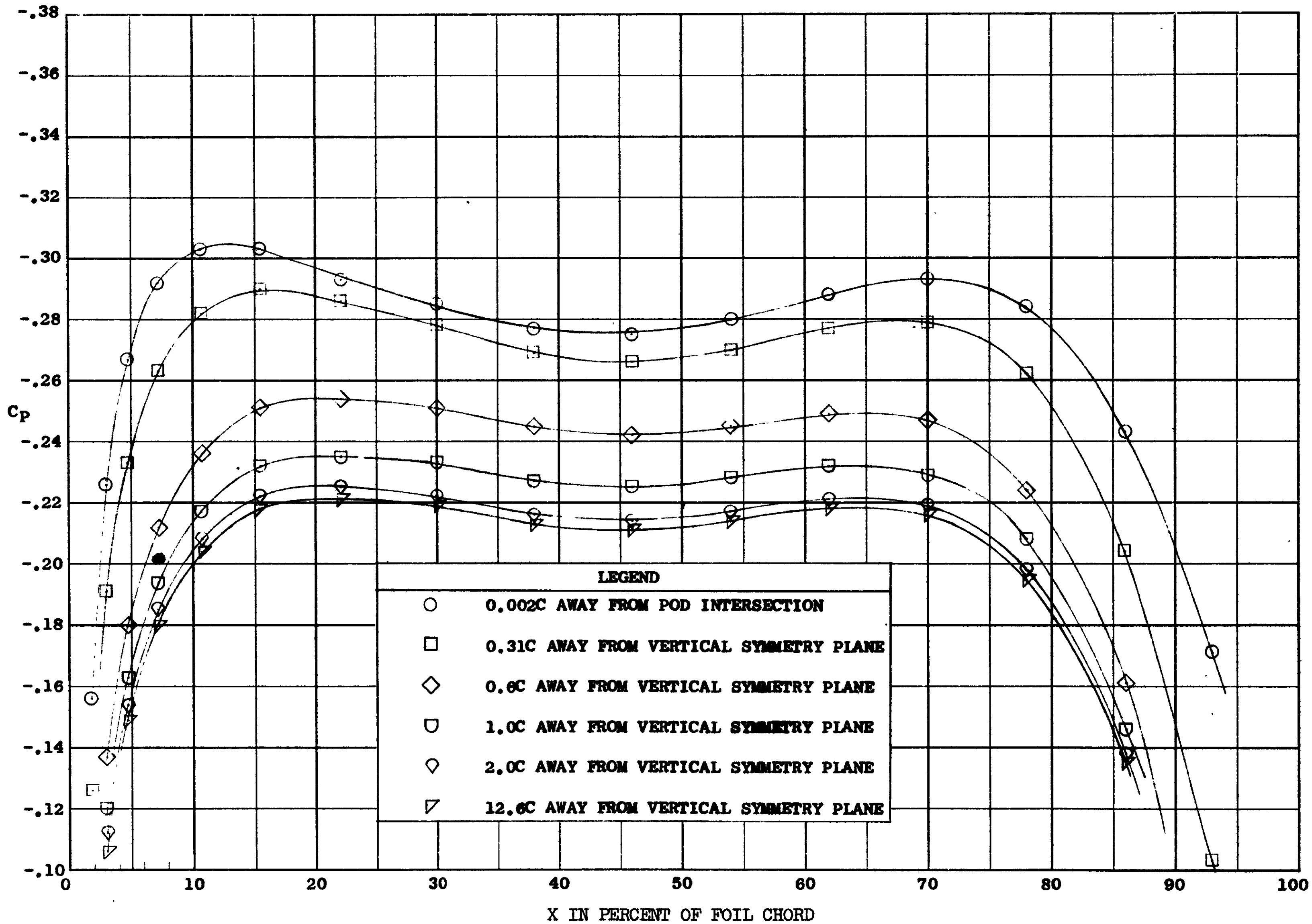

Figure 7 - Potential Flow Pressure Distribution on Foil Upper Surface of Pod-Foil Configuration at Zero Lift

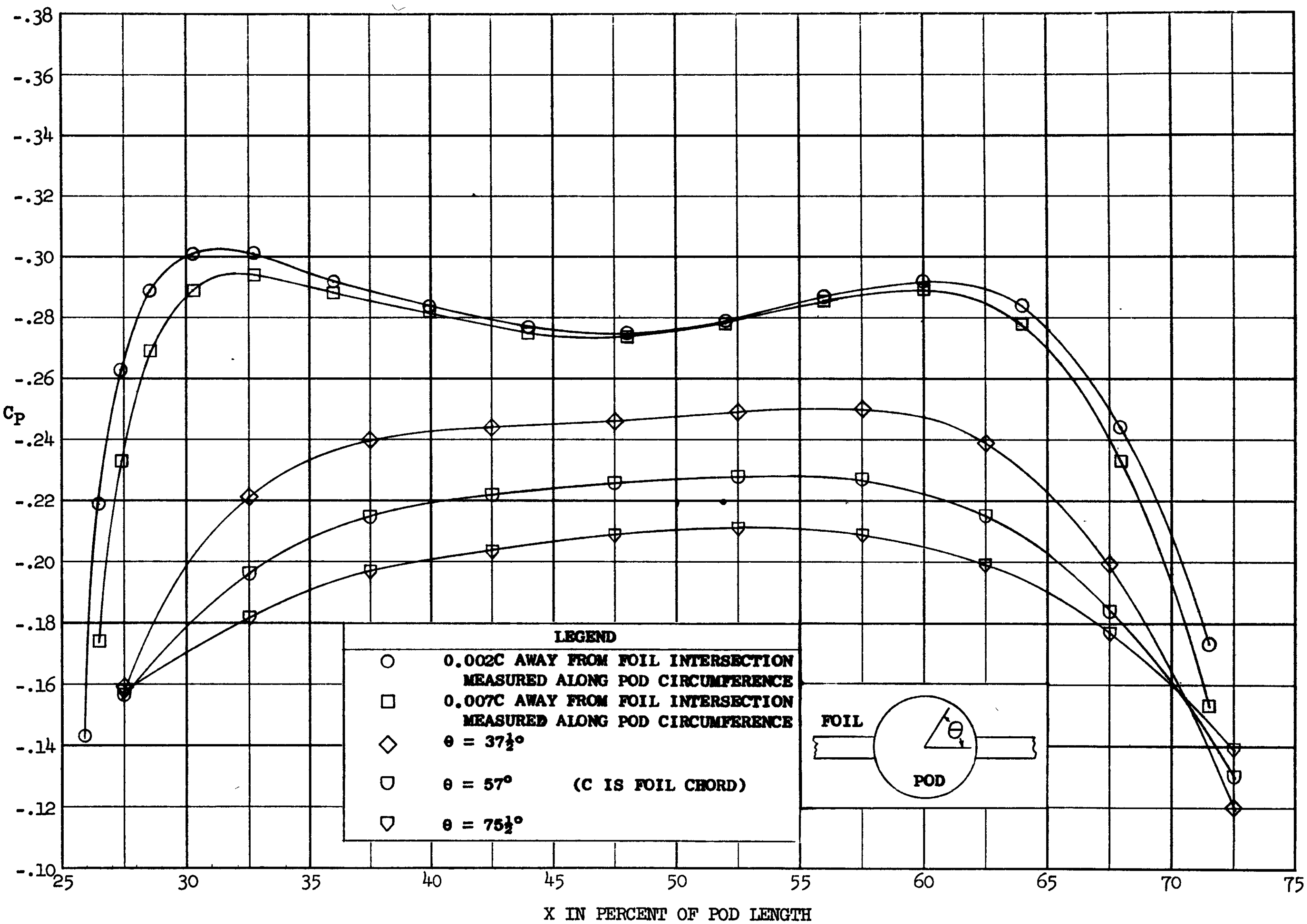

Figure 8 - Potential Flow Pressure Distribution on Pod Surface of Pod-Foil Configuration at Zero Lift

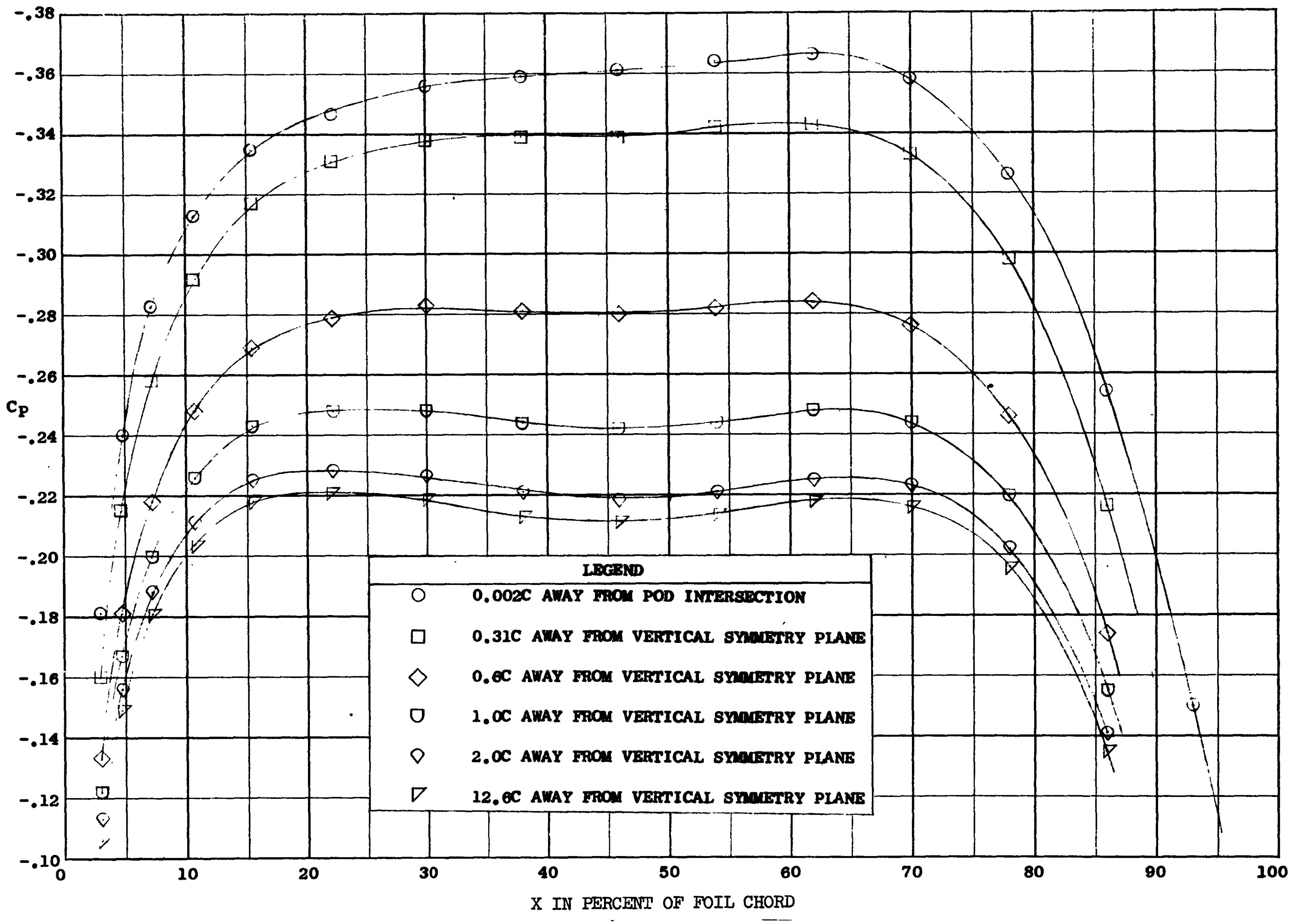

Figure 9 - Potential Flow Pressure Distribution on Foil Upper Surface of Strut-Pod-Foil Configuration at Zero Lift

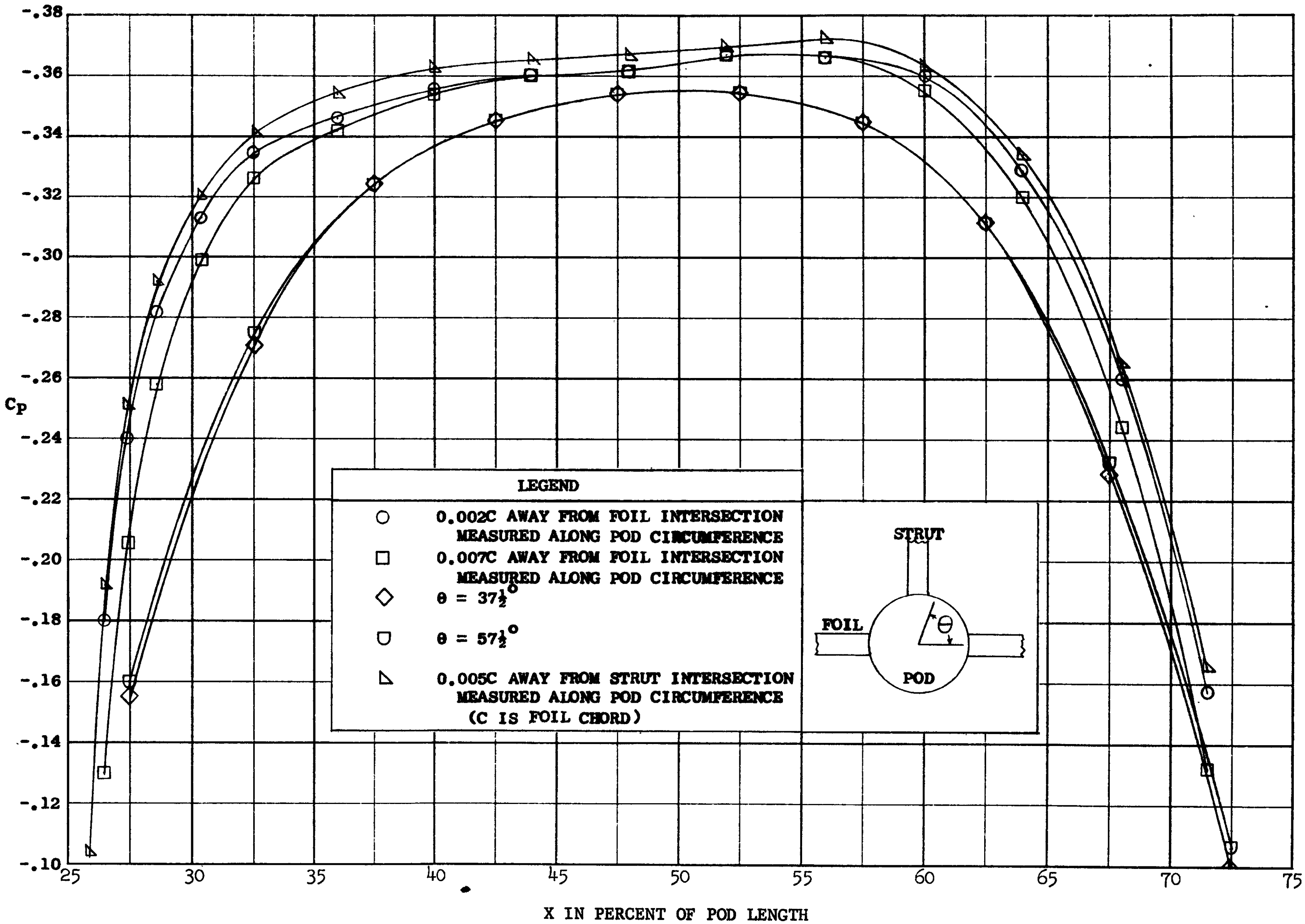

Figure 10 - Potential Flow Pressure Distribution on Pod Upper Surface of Strut-Pod-Foil Configuration at Zero Lift

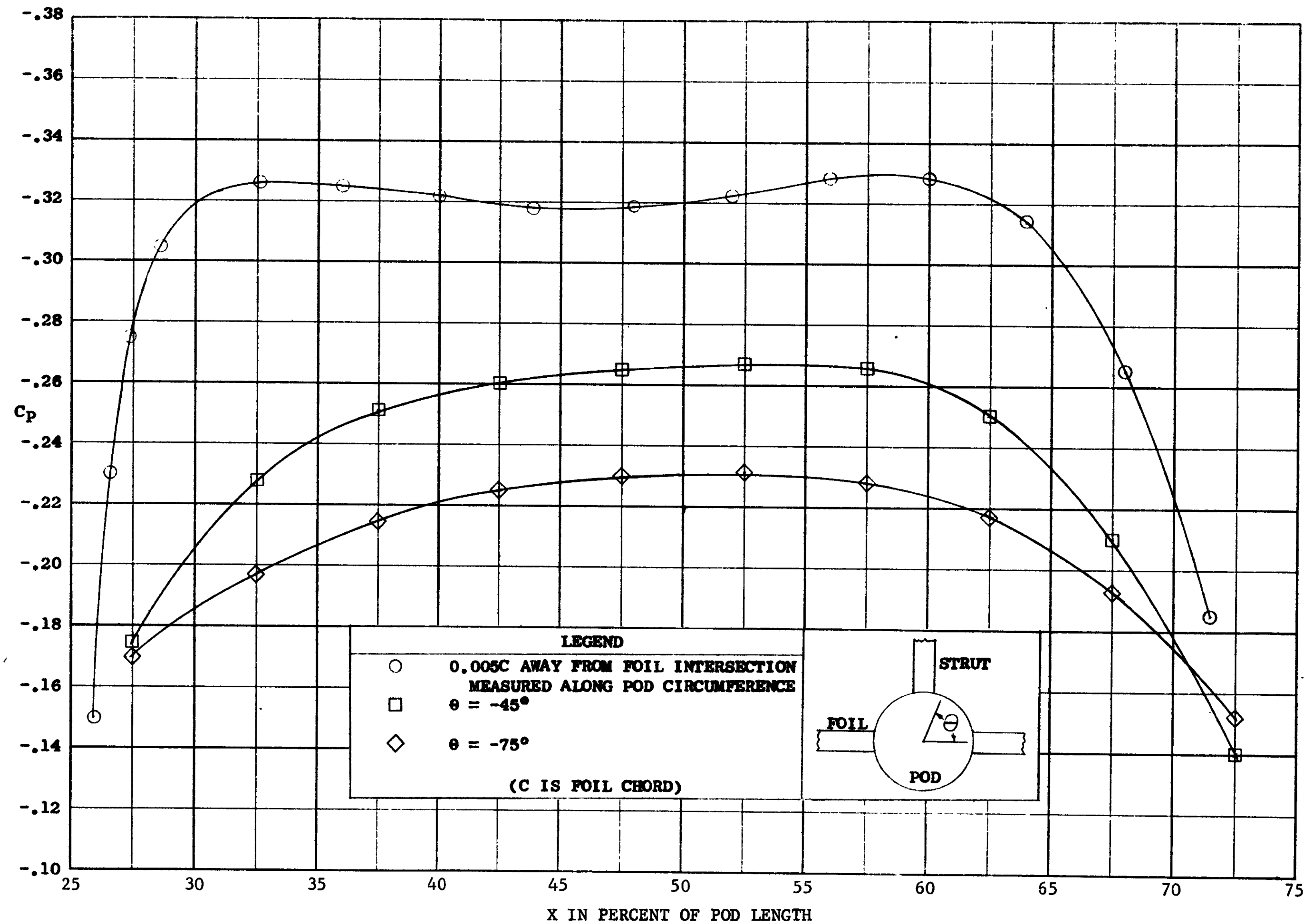

Figure 11 - Potential Flow Pressure Distribution on Pod Lower Surface of Strut-Pod-Foil Configuration at Zero Lift

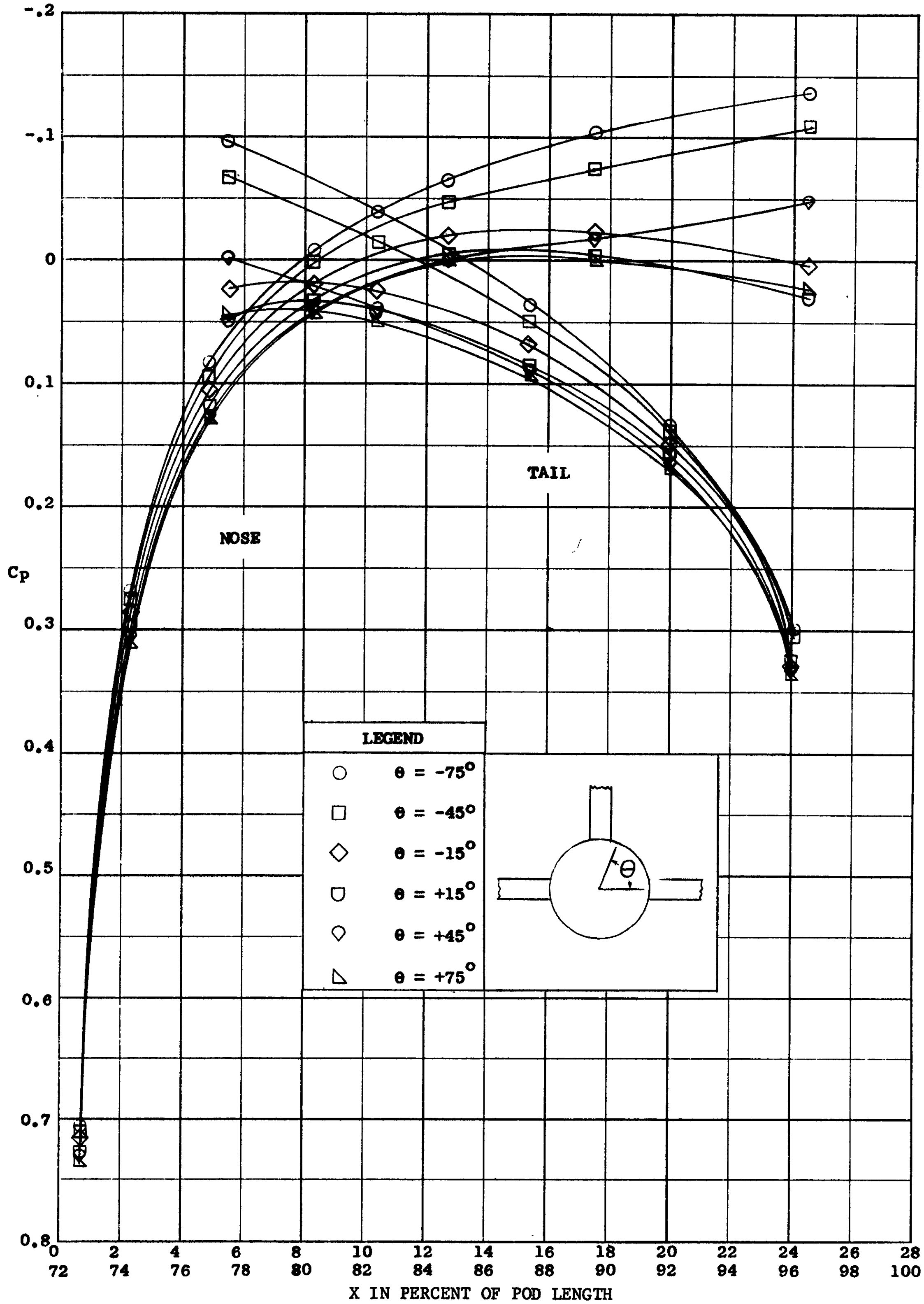

Figure 12 - Potential Flow Pressure Distributions on Pod Nose and Tail Surfaces of Strut-Pod-Foil Configuration at Zero Lift

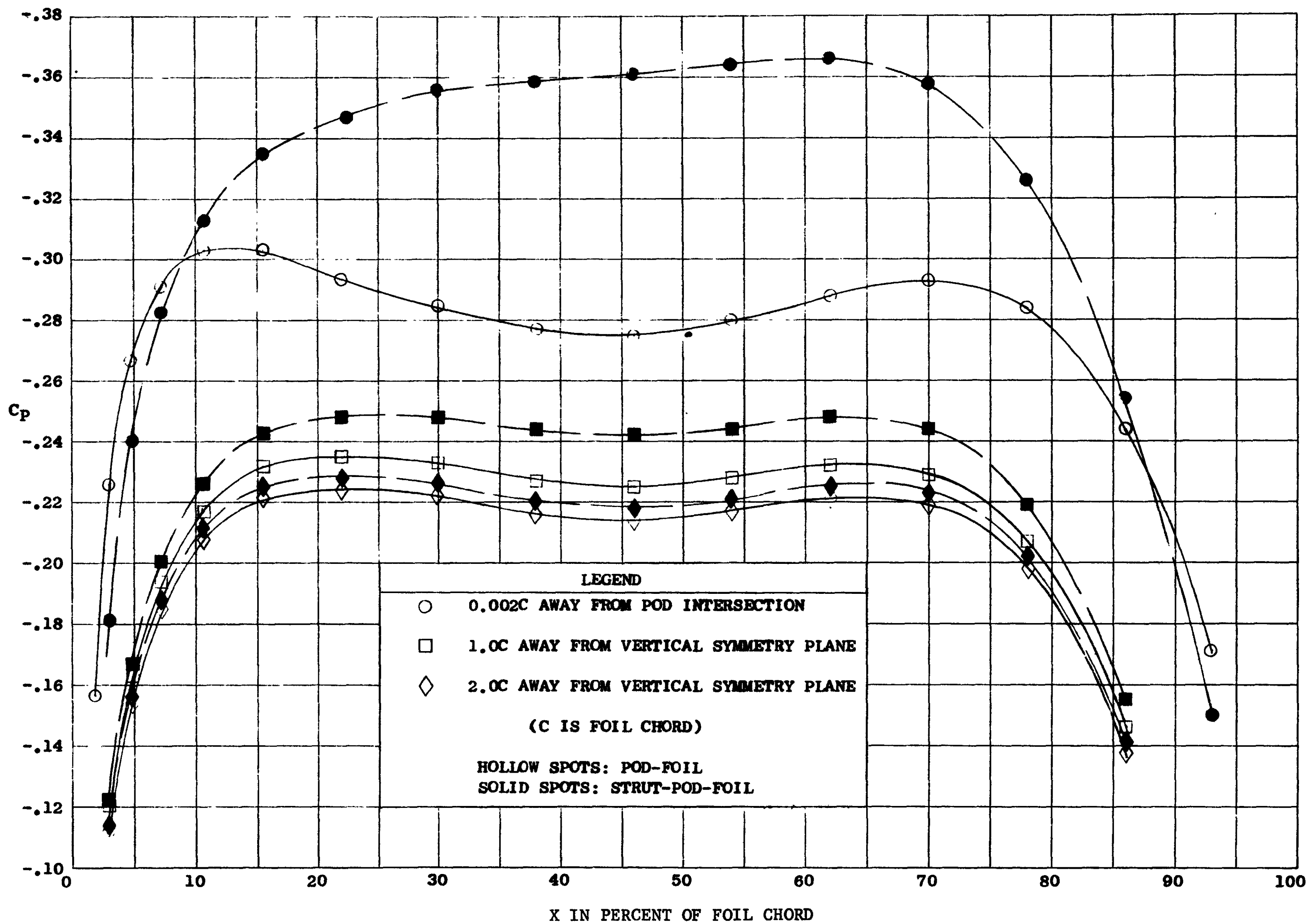

Figure 13 - Potential Flow Pressure Distributions on Foil Upper Surface of Pod-Foil Configuration at Zero Lift with and without Strut

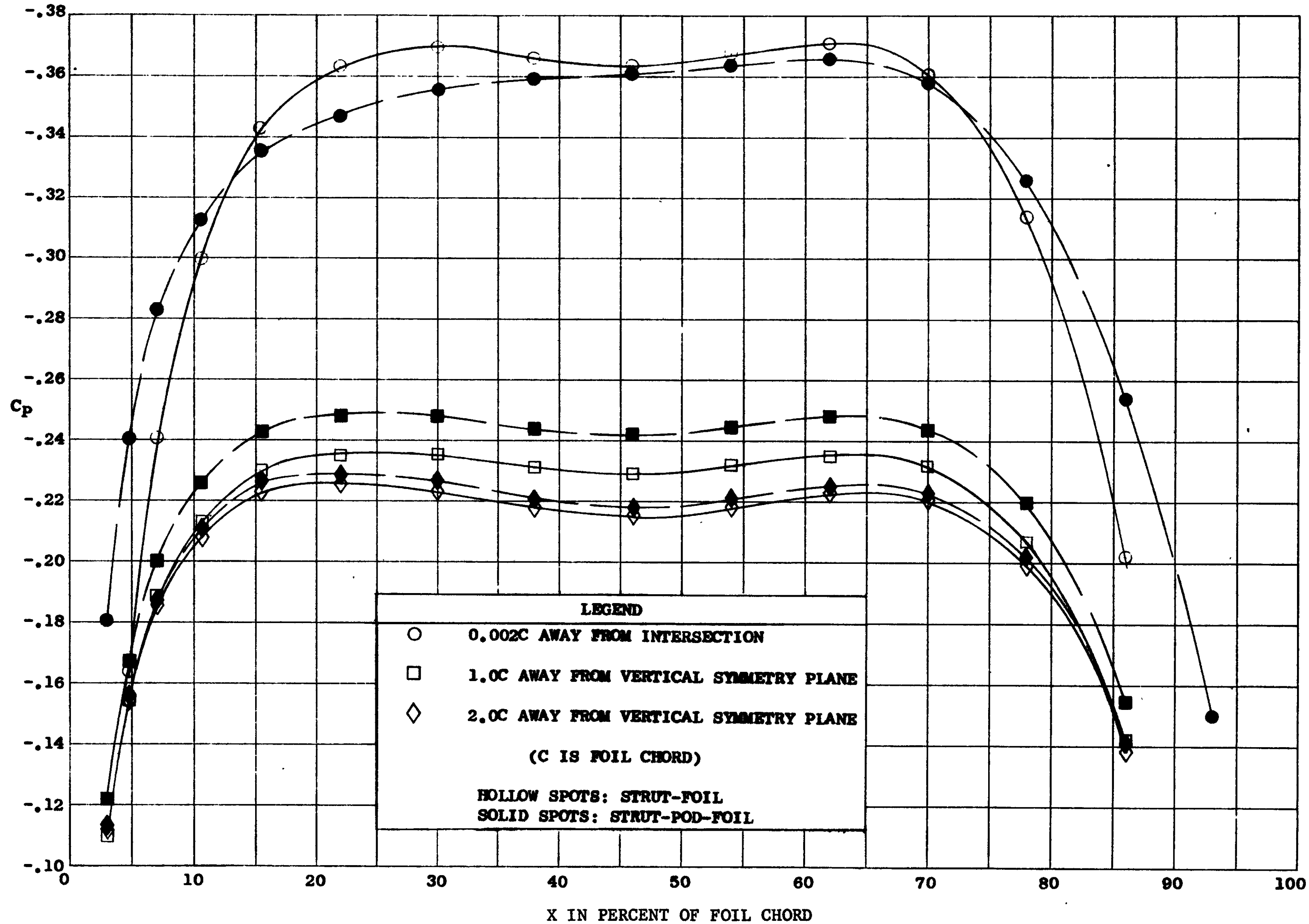

Figure 14 - Potential Flow Pressure Distributions on Foil Upper Surface of Strut-Foil Configuration

TABLE 1

Offsets for Crossed-Foil Model

Axial Offsets	Transverse Offsets	
	Thin Foil	Thick Foil
000.0000000	000.0000000	000.0000000
000.1400000	000.3742789	000.7485578
000.6000000	000.7755068	001.5510136
001.3000000	001.1426344	002.2852688
002.3000000	001.5209316	003.0418633
003.7400000	001.9389202	003.8778403
005.7800000	002.4037375	004.8074751
008.6400000	002.9157333	005.8314667
012.6600000	003.4678836	006.9357671
018.2600000	004.0251906	008.0503812
026.0000000	004.5254947	009.0509894
034.0000000	004.8228269	009.6456538
042.0000000	004.9685367	009.9370733
050.0000000	004.9964460	009.9928919
058.0000000	004.9055322	009.8110644
066.0000000	004.6638045	009.3276089
074.0000000	004.2146215	008.4292431
082.0000000	003.4837887	006.9675775
090.0000000	002.3836441	004.7672881
096.0000000	001.2448203	002.4896407
100.0000000	000.0000000	000.0000000

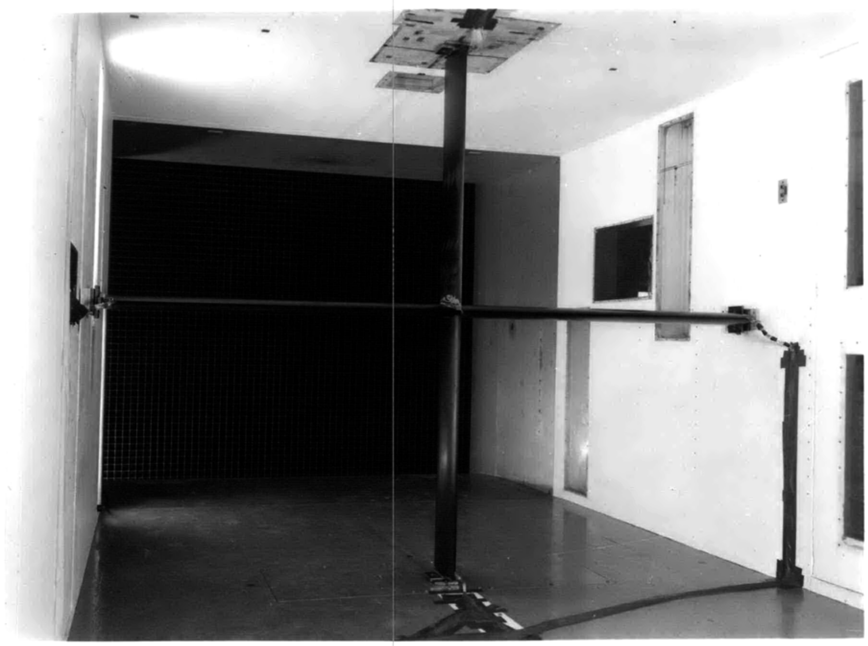

Figure 15 - Crossed Foil Model in TMB Wind Tunnel

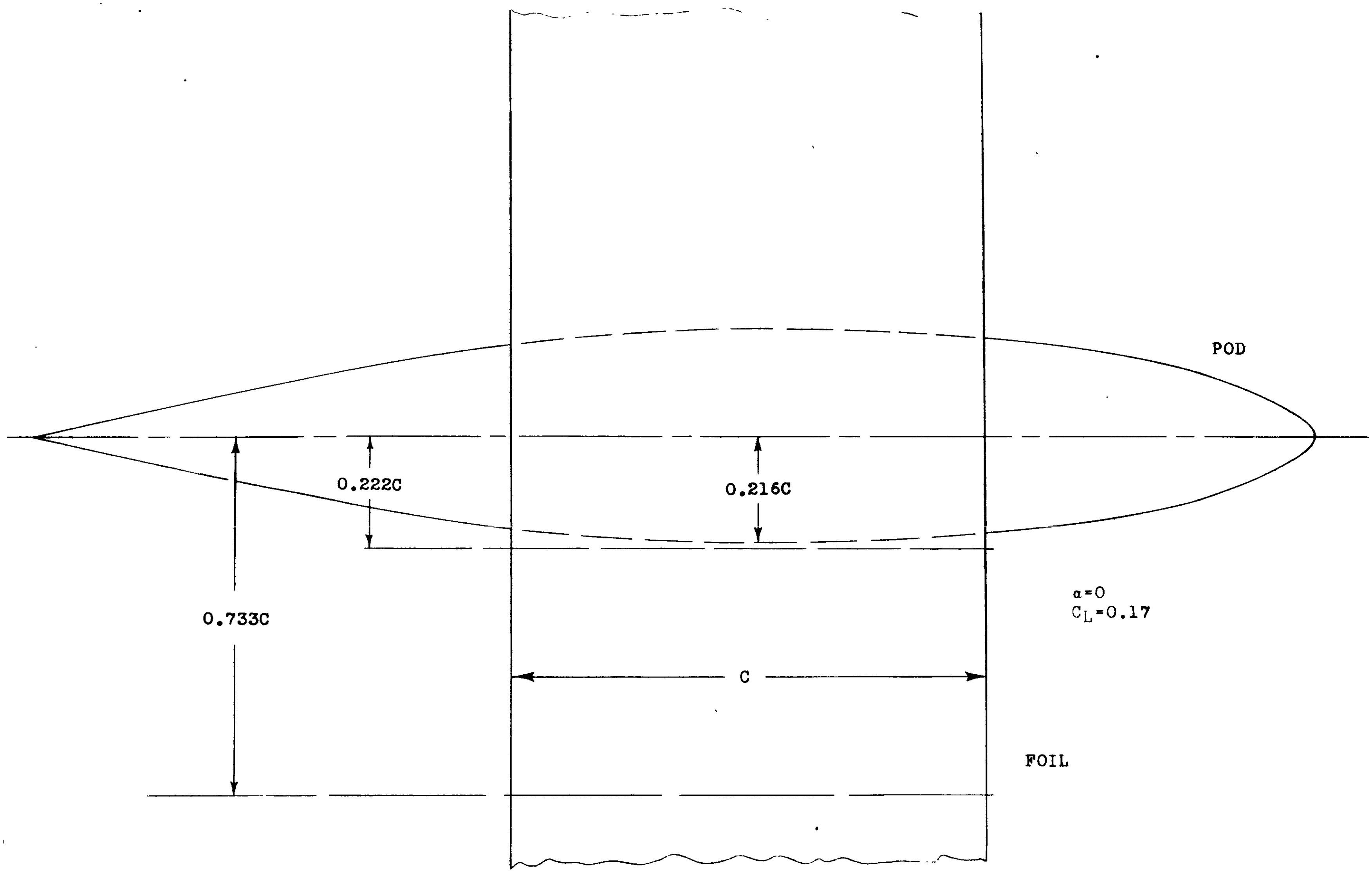

Figure 16 - Spanwise Positions at which Theoretical and Experimental Pressures are Compared on NACA Pod-Foil with Lift.

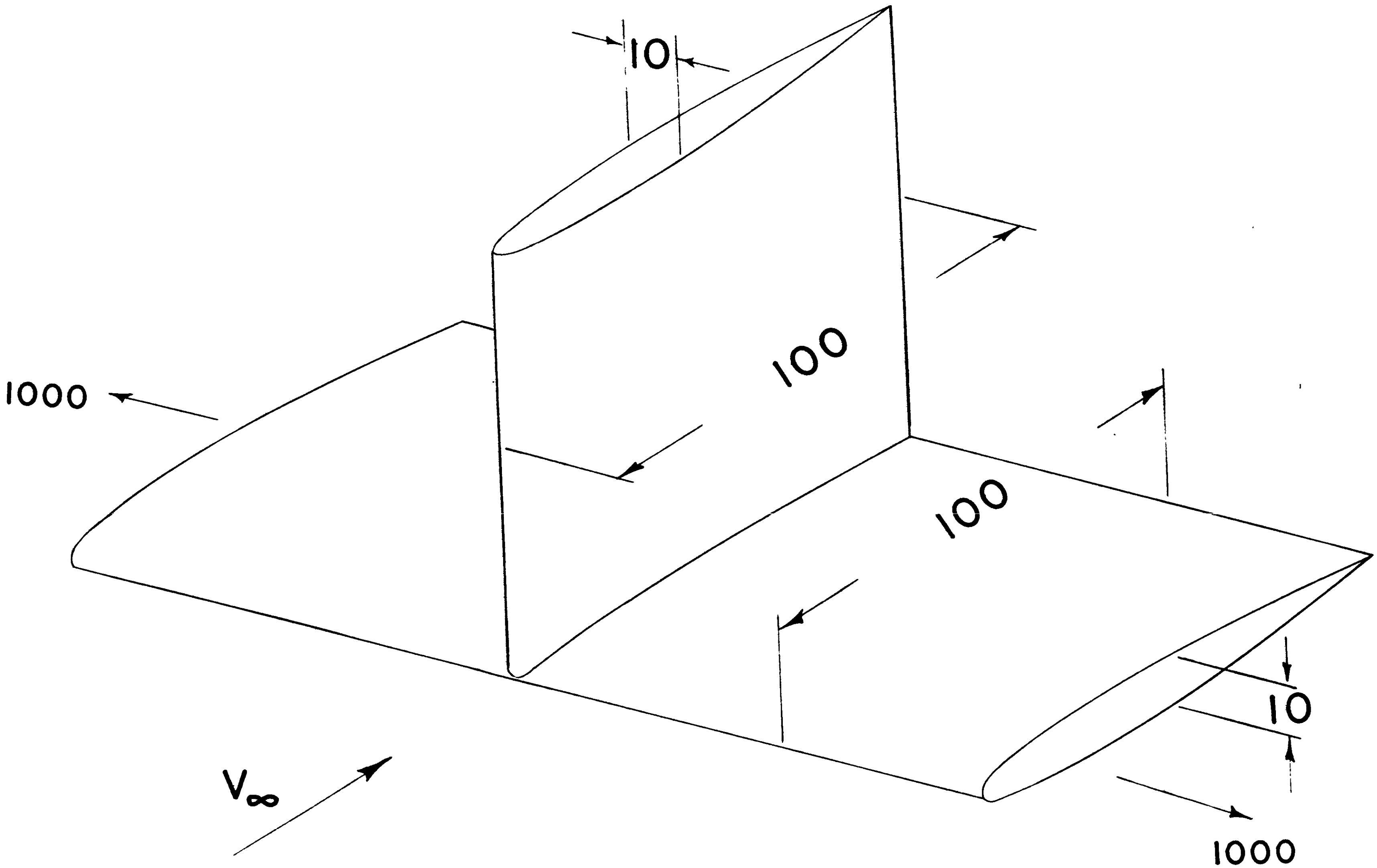

Figure 17 – Strut-Foil Configuration

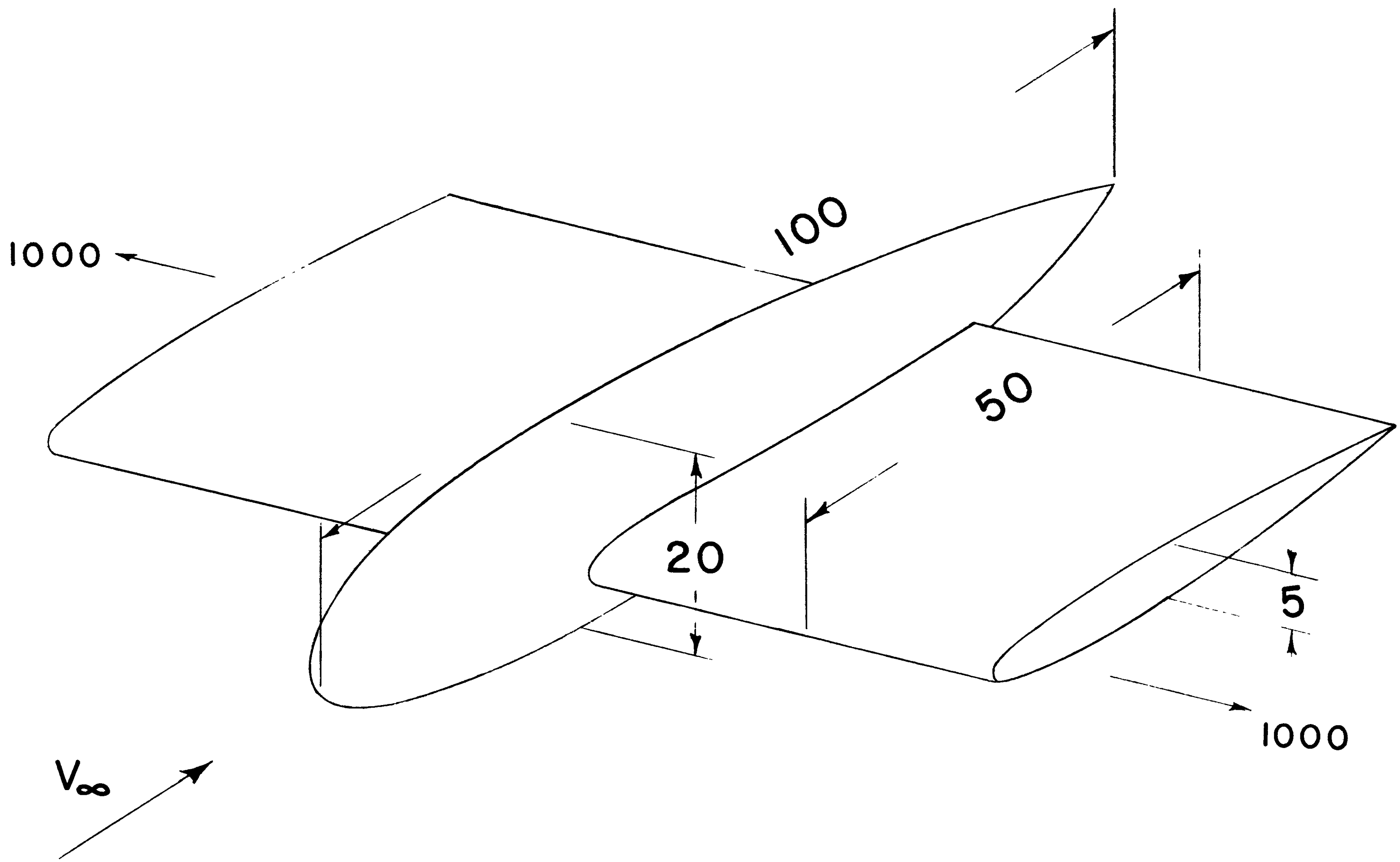

Figure 18 - Pod-Foil Configuration

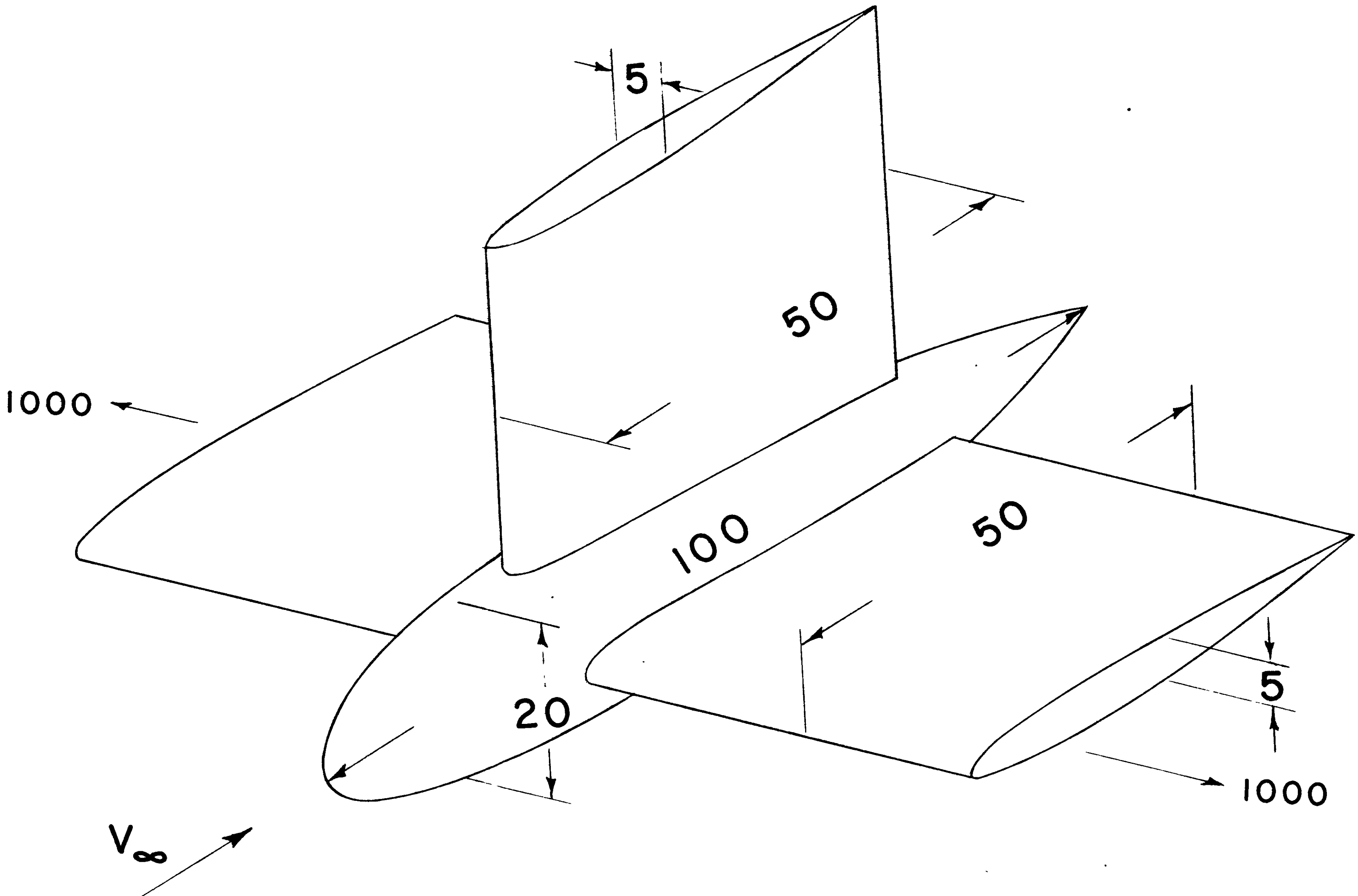

Figure 19 - Strut-Pod-Foil Configuration

TABLE 2

NACA Pod Ordinates

[**Stations and radii in percent of pod length**]

Station	Radius	Station	Radius
0	0		
1.25	1.583	50.00	8.217
2.50	2.392	55.00	7.933
5.00	3.592	60.00	7.483
7.50	4.467	65.00	6.833
10.00	5.167	70.00	6.033
15.00	6.183	75.00	5.100
20.00	6.925	80.00	4.092
25.00	7.483	85.00	3.092
30.00	7.900	90.00	2.075
35.00	8.183	95.00	1.033
40.00	8.333	97.50	.520
45.00	8.333	100.00	0

TABLE 3

NACA 65-210 Airfoil Ordinates

[Stations and ordinates given in percent of airfoil chord]

Upper surface		Lower surface	
Station	Ordinate	Station	Ordinate
0	0	0	0
.435	.819	.565	- .719
.678	.999	.822	- .859
1.169	1.273	1.331	-1.059
2.408	1.757	2.592	-1.385
4.898	2.491	5.102	-1.859
7.394	3.069	7.606	-2.221
9.894	3.555	10.106	-2.521
14.899	4.338	15.101	-2.992
19.909	4.938	20.091	-3.346
24.921	5.397	25.079	-3.607
29.936	5.732	30.064	-3.788
34.951	5.954	35.049	-3.894
39.968	6.067	40.032	-3.925
44.984	6.058	45.016	-3.868
50.000	5.915	50.000	-3.709
55.014	5.625	54.986	-3.435
60.027	5.217	59.973	-3.075
65.036	4.712	64.964	-2.652
70.043	4.128	69.957	-2.184
75.045	3.479	74.955	-1.689
80.044	2.783	79.956	-1.191
85.038	2.057	84.962	- .711
90.028	1.327	89.972	- .293
95.014	.622	94.986	.010
[a]100.000	0	[a]100.000	0

L. E. radius: 0.687
Slope of radius through L. E.: 0.084

[a]2.22 percent of the chord was removed at the trailing edge for experimental model.

TABLE 4

TMB Series 58 Pod Offsets

(Stations and radii in percent of pod length)

Station	Radius	Station	Radius
0	0		
0.99	1.9935016	50.00	9.9928919
3.20	3.5879770	55.00	9.9099350
6.27	5.0019025	60.00	9.7221735
10.18	6.2924278	65.00	9.4080154
15.00	7.4514705	70.00	8.9388922
20.00	8.3218400	75.00	8.2806816
25.00	8.9490522	80.00	7.3949167
30.00	9.3933284	85.00	6.2394310
35.00	9.6965789	90.00	4.7672881
40.00	9.8877164	95.00	2.9160162
45.00	9.9842616	100.00	0

TABLE 5

Strut-Pod-Foil Offsets

	X	Y	Z
POD NOSE	000.0000000	000.0000000	-000.0000000
	000.9900000	000.0000000	-001.9935016
	003.2000000	000.0000000	-003.5879770
	006.2700000	000.0000000	-005.0019025
	010.1800000	000.0000000	-006.2924278
	015.0000000	000.0000000	-007.4514705
	020.0000000	000.0000000	-008.3218400
	025.0000000	000.0000000	-008.9490522
	000.0000000	000.0000000	-000.0000000
	000.9900000	000.9967508	-001.7264230
	003.2000000	001.7939885	-003.1072792
	006.2700000	002.5009512	-004.3317746
	010.1800000	003.1462139	-005.4494023
	015.0000000	003.7257352	-006.4531628
	020.0000000	004.1609200	-007.2069248
	025.0000000	004.4745261	-007.7501065
	000.0000000	000.0000000	-000.0000000
	000.9900000	001.7264230	-000.9967508
	003.2000000	003.1072792	-001.7939885
	006.2700000	004.3317746	-002.5009512
	010.1800000	005.4494023	-003.1462139
	015.0000000	006.4531628	-003.7257352
	020.0000000	007.2069248	-004.1609200
	025.0000000	007.7501065	-004.4745261
	000.0000000	000.0000000	000.0000000
	000.9900000	001.9935016	000.0000000
	003.2000000	003.5879770	000.0000000
	006.2700000	005.0019025	000.0000000
	010.1800000	006.2924278	000.0000000
	015.0000000	007.4514705	000.0000000
	020.0000000	008.3218400	000.0000000
	025.0000000	008.9490522	000.0000000
	000.0000000	000.0000000	000.0000000
	000.9900000	001.7264230	000.9967508
	003.2000000	003.1072792	001.7939885
	006.2700000	004.3317746	002.5009512
	010.1800000	005.4494023	003.1462139
	015.0000000	006.4531628	003.7257352
	020.0000000	007.2069248	004.1609200
	025.0000000	007.7501065	004.4745261
	000.0000000	000.0000000	000.0000000
	000.9900000	000.9967508	001.7264230
	003.2000000	001.7939885	003.1072792
	006.2700000	002.5009512	004.3317746
	010.1800000	003.1462139	005.4494023
	015.0000000	003.7257352	006.4531628
	020.0000000	004.1609200	007.2069248
	025.0000000	004.4745261	007.7501065
	000.0000000	000.0000000	000.0000000
	000.9900000	000.0000000	001.9935016
	003.2000000	000.0000000	003.5879770
	006.2700000	000.0000000	005.0019025
	010.1800000	000.0000000	006.2924278
	015.0000000	000.0000000	007.4514705
	020.0000000	000.0000000	008.3218400

	X	Y	Z
POD TAIL	025.0000000	000.0000000	008.9490522
	075.0000000	000.0000000	-008.2806816
	080.0000000	000.0000000	-007.3949167
	085.0000000	000.0000000	-006.2394310
	090.0000000	000.0000000	-004.7672881
	095.0000000	000.0000000	-002.9160162
	100.0000000	000.0000000	-000.0000000
	075.0000000	004.1403408	-007.1712806
	080.0000000	003.6974584	-006.4041857
	085.0000000	003.1197155	-005.4035058
	090.0000000	002.3836440	-004.1285926
	095.0000000	001.4580081	-002.5253441
	100.0000000	000.0000000	-000.0000000
	075.0000000	007.1712806	-004.1403408
	080.0000000	006.4041857	-003.6974584
	085.0000000	005.4035058	-003.1197155
	090.0000000	004.1285926	-002.3836440
	095.0000000	002.5253441	-001.4580081
	100.0000000	000.0000000	-000.0000000
	075.0000000	008.2806816	000.0000000
	080.0000000	007.3949167	000.0000000
	085.0000000	006.2394310	000.0000000
	090.0000000	004.7672881	000.0000000
	095.0000000	002.9160162	000.0000000
	100.0000000	000.0000000	000.0000000
	075.0000000	007.1712806	004.1403408
	080.0000000	006.4041857	003.6974584
	085.0000000	005.4035058	003.1197155
	090.0000000	004.1285926	002.3836440
	095.0000000	002.5253441	001.4580081
	100.0000000	000.0000000	000.0000000
	075.0000000	004.1403408	007.1712806
	080.0000000	003.6974584	006.4041857
	085.0000000	003.1197155	005.4035058
	090.0000000	002.3836440	004.1285926
	095.0000000	001.4580081	002.5253441
	100.0000000	000.0000000	000.0000000
	075.0000000	000.0000000	008.2806816
	080.0000000	000.0000000	007.3949167
	085.0000000	000.0000000	006.2394310
	090.0000000	000.0000000	004.7672881
	095.0000000	000.0000000	002.9160162
	100.0000000	000.0000000	000.0000000
LOWER SURFACE OF POD	025.0000000	000.0000000	-008.9490522
	030.0000000	000.0000000	-009.3933284
	035.0000000	000.0000000	-009.6965789
	040.0000000	000.0000000	-009.8877164
	045.0000000	000.0000000	-009.9842616
	050.0000000	000.0000000	-009.9928919
	055.0000000	000.0000000	-009.9099350
	060.0000000	000.0000000	-009.7221735
	065.0000000	000.0000000	-009.4080154
	070.0000000	000.0000000	-008.9388922
	075.0000000	000.0000000	-008.2806816
	025.0000000	004.4745259	-007.7501064
	030.0000000	004.6966640	-008.1348609
	035.0000000	004.8482893	-008.3974836
	040.0000000	004.9438580	-008.5630134
	045.0000000	004.9921306	-008.6466241
	050.0000000	004.9964457	-008.6540980

	X	Y	Z
	055.0000000	004.9549673	-008.5822554
	060.0000000	004.8610865	-008.4196491
	065.0000000	004.7040075	-008.1475803
	070.0000000	004.4694459	-007.7413076
	075.0000000	004.1403406	-007.1712805
	025.0000000	007.7501063	-004.4745260
	030.0000000	008.1348608	-004.6966642
	035.0000000	008.3974835	-004.8482894
	040.0000000	008.5630133	-004.9438581
	045.0000000	008.6466238	-004.9921308
	050.0000000	008.6540979	-004.9964459
	055.0000000	008.5822552	-004.9549675
	060.0000000	008.4196490	-004.8610867
	065.0000000	008.1475801	-004.7040077
	070.0000000	007.7413075	-004.4694461
	075.0000000	007.1712804	-004.1403407
LOWER SURFACE OF POD NEAR FOIL	025.0000000	007.7501063	-004.4745260
	025.0700000	007.7564867	-004.4782098
	025.3000000	007.7772350	-004.4901888
	025.6500000	007.8081827	-004.5080565
	026.1500000	007.8511063	-004.5328385
	026.8700000	007.9103293	-004.5670308
	027.8900000	007.9892033	-004.6125688
	029.3200000	008.0903898	-004.6709889
	031.3300000	008.2154255	-004.7431782
	034.1300000	008.3593377	-004.8262660
	038.0000000	008.5072674	-004.9116732
	042.0000000	008.6057576	-004.9685366
	046.0000000	008.6541857	-004.9964966
	050.0000000	008.6540979	-004.9964459
	054.0000000	008.6034065	-004.9671792
	058.0000000	008.4966308	-004.9055322
	062.0000000	008.3252212	-004.8065688
	066.0000000	008.0779459	-004.6638044
	070.0000000	007.7413075	-004.4694461
	073.0000000	007.4209999	-004.2845164
	075.0000000	007.1712804	-004.1403407
	025.0000000	008.5760514	-002.5567314
	025.0700000	008.5559700	-002.6481748
	025.3000000	008.5489292	-002.7500891
	025.6500000	008.5549133	-002.8467084
	026.1500000	008.5724895	-002.9493932
	026.8700000	008.6040338	-003.0662163
	027.8900000	008.6523973	-003.1998724
	029.3200000	008.7201838	-003.3512592
	031.3300000	008.8094287	-003.5192219
	034.1300000	008.9176917	-003.6940691
	038.0000000	009.0345939	-003.8567144
	042.0000000	009.1154149	-003.9565937
	046.0000000	009.1550565	-004.0056022
	050.0000000	009.1520671	-004.0121755
	054.0000000	009.1042495	-003.9754393
	058.0000000	009.0085757	-003.8861994
	062.0000000	008.8606051	-003.7285507
	066.0000000	008.6534532	-003.4816709
	070.0000000	008.3764415	-003.1207402
	073.0000000	008.1140703	-002.7550289
	075.0000000	007.9301842	-002.3836662
	025.0000000	008.9350877	-000.4997399
	025.0700000	008.9300725	-000.6864794

TABLE 5 - CONTINUED

	X	Y	Z
	025.3000000	008.9365220	-000.8864286
	025.6500000	008.9524939	-001.0691783
	026.1500000	008.9780681	-001.2572945
	026.8700000	009.0158219	-001.4649355
	027.8900000	009.0679712	-001.6956001
	029.3200000	009.1363184	-001.9494179
	031.3300000	009.2222420	-002.2228832
	034.1300000	009.3235149	-002.4986879
	038.0000000	009.4316877	-002.7461612
	042.0000000	009.5065635	-002.8932115
	046.0000000	009.5429106	-002.9652600
	050.0000000	009.5385188	-002.9790171
	054.0000000	009.4912201	-002.9339763
	058.0000000	009.3987496	-002.8143359
	062.0000000	009.2570803	-002.5920797
	066.0000000	009.0570289	-002.2303615
	070.0000000	008.7785974	-001.6852358
	073.0000000	008.4955570	-001.1197471
	075.0000000	008.2655905	-000.4996962
	025.0000000	008.9490520	-000.0000000
	025.0700000	008.9544642	-000.1871395
	025.3000000	008.9720025	-000.3877534
	025.6500000	008.9979935	-000.5713172
	026.1500000	009.0337250	-000.7604658
	026.8700000	009.0824682	-000.9694601
	027.8900000	009.1465114	-001.2018688
	029.3200000	009.2275224	-001.4578667
	031.3300000	009.3265430	-001.7339418
	034.1300000	009.4403831	-002.0125953
	038.0000000	009.5591898	-002.2627473
	042.0000000	009.6400471	-002.4114135
	046.0000000	009.6792728	-002.4842683
	050.0000000	009.6755757	-002.4982230
	054.0000000	009.6268071	-002.4527661
	058.0000000	009.5299115	-002.3319022
	062.0000000	009.3793206	-002.1073108
	066.0000000	009.1635194	-001.7418944
	070.0000000	008.8590831	-001.1918220
	073.0000000	008.5463985	-000.6224102
	075.0000000	008.2806814	-000.0000000
UPPER	025.0000000	008.9490520	000.0000000
SURFACE	025.0700000	008.9544642	000.1871395
OF POD	025.3000000	008.9720025	000.3877534
NEAR FOIL	025.6500000	008.9979935	000.5713172
	026.1500000	009.0337250	000.7604658
	026.8700000	009.0824682	000.9694601
	027.8900000	009.1465114	001.2018688
	029.3200000	009.2275224	001.4578667
	031.3300000	009.3265430	001.7339418
	034.1300000	009.4403831	002.0125953
	038.0000000	009.5591898	002.2627473
	042.0000000	009.6400471	002.4114135
	046.0000000	009.6792728	002.4842683
	050.0000000	009.6755757	002.4982230
	054.0000000	009.6268071	002.4527661
	058.0000000	009.5299115	002.3319022
	062.0000000	009.3793206	002.1073108
	066.0000000	009.1635194	001.7418944
	070.0000000	008.8590831	001.1918220
	073.0000000	008.5463985	000.6224102
	075.0000000	008.2806814	000.0000000
	025.0000000	008.9468172	000.1999833
	025.0700000	008.9480531	000.3870328
	025.3000000	008.9611427	000.5874546
	025.6500000	008.9831076	000.7707584
	026.1500000	009.0147513	000.9595595
	026.8700000	009.0590653	001.1680822
	027.8900000	009.1183077	001.3998666
	029.3200000	009.1941991	001.6550676
	031.3300000	009.2879164	001.9301728
	034.1300000	009.3966588	002.2077537
	038.0000000	009.5111431	002.4568866
	042.0000000	009.5895642	002.6049337
	046.0000000	009.6276174	002.6774788
	050.0000000	009.6236414	002.6913587
	054.0000000	009.5754802	002.6460641
	058.0000000	009.4803988	002.5256728
	062.0000000	009.3334516	002.3019760
	066.0000000	009.1240666	001.9379608
	070.0000000	008.8302019	001.3897218
	073.0000000	008.5295451	000.8216941
	075.0000000	008.2782662	000.1999805
	025.0000000	008.9350877	000.4997399
	025.0700000	008.9300725	000.6864794
	025.3000000	008.9365220	000.8864286
	025.6500000	008.9524939	001.0691783
	026.1500000	008.9780681	001.2572945
	026.8700000	009.0158219	001.4649355
	027.8900000	009.0679712	001.6956001
	029.3200000	009.1363184	001.9494179
	031.3300000	009.2222420	002.2228832
	034.1300000	009.3235149	002.4986879
	038.0000000	009.4316877	002.7461612
	042.0000000	009.5065635	002.8932115
	046.0000000	009.5429106	002.9652600
	050.0000000	009.5385188	002.9790171
	054.0000000	009.4912201	002.9339763
	058.0000000	009.3987496	002.8143359
	062.0000000	009.2570803	002.5920797
	066.0000000	009.0570289	002.2303615
	070.0000000	008.7785974	001.6852358
	073.0000000	008.4955570	001.1197471
	075.0000000	008.2655905	000.4996962
	025.0000000	008.5760514	002.5567314
	025.0700000	008.5559700	002.6481748
	025.3000000	008.5489292	002.7500891
	025.6500000	008.5549133	002.8467084
	026.1500000	008.5724895	002.9493932
	026.8700000	008.6040338	003.0662163
	027.8900000	008.6523973	003.1998724
	029.3200000	008.7201838	003.3512592
	031.3300000	008.8094287	003.5192219
	034.1300000	008.9176917	003.6940691
	038.0000000	009.0345939	003.8567144
	042.0000000	009.1154149	003.9565937
	046.0000000	009.1550565	004.0056022
	050.0000000	009.1520671	004.0121755
	054.0000000	009.1042495	003.9754393
	058.0000000	009.0085757	003.8861994
	062.0000000	008.8606051	003.7285507
	066.0000000	008.6534532	003.4816709
	070.0000000	008.3764415	003.1207402
	073.0000000	008.1140703	002.7550289
	075.0000000	007.9301842	002.3836662
	025.0000000	007.7501063	004.4745260
	025.0700000	007.7564867	004.4782098
	025.3000000	007.7772350	004.4901888
	025.6500000	007.8081827	004.5080565
	026.1500000	007.8511063	004.5328385
	026.8700000	007.9103293	004.5670308
	027.8900000	007.9892033	004.6125688
	029.3200000	008.0903898	004.6709889
	031.3300000	008.2154255	004.7431782
	034.1300000	008.3593377	004.8262660
	038.0000000	008.5072674	004.9116732
	042.0000000	008.6057576	004.9685366
	046.0000000	008.6541857	004.9964966
	050.0000000	008.6540979	004.9964459
	054.0000000	008.6034065	004.9671792
	058.0000000	008.4966308	004.9055322
	062.0000000	008.3252212	004.8065688
	066.0000000	008.0779459	004.6638044
	070.0000000	007.7413075	004.4694461
	073.0000000	007.4209999	004.2845164
	075.0000000	007.1712804	004.1403407
MIDDLE	025.0000000	007.7501063	004.4745260
PART OF	030.0000000	008.1348608	004.6966642
UPPER	035.0000000	008.3974835	004.8482894
SURFACE	040.0000000	008.5630133	004.9438581
OF POD	045.0000000	008.6466238	004.9921308
	050.0000000	008.6540979	004.9964459
	055.0000000	008.5822552	004.9549675
	060.0000000	008.4196490	004.8610867
	065.0000000	008.1475801	004.7040077
	070.0000000	007.7413075	004.4694461
	075.0000000	007.1712804	004.1403407
	025.0000000	006.3279355	006.3279355
	030.0000000	006.6420862	006.6420862
	035.0000000	006.8565167	006.8565167
	040.0000000	006.9916713	006.9916713
	045.0000000	007.0599391	007.0599391
	050.0000000	007.0660416	007.0660416
	055.0000000	007.0073822	007.0073822
	060.0000000	006.8746148	006.8746148
	065.0000000	006.6524715	006.6524715
	070.0000000	006.3207513	006.3207513
	075.0000000	005.8553261	005.8553261
	025.0000000	004.4745259	007.7501064
	030.0000000	004.6966640	008.1348609
	035.0000000	004.8482893	008.3974836
	040.0000000	004.9438580	008.5630134
	045.0000000	004.9921306	008.6466241
	050.0000000	004.9964457	008.6540980
	055.0000000	004.9549673	008.5822554
	060.0000000	004.8610865	008.4196491
	065.0000000	004.7040075	008.1475803
	070.0000000	004.4694459	007.7413076
	075.0000000	004.1403406	007.1712805
	025.0000000	004.4745260	007.7501063
	025.0700000	004.4782098	007.7564867

TABLE 5 - CONTINUED

	X	Y	Z
UPPER SURFACE OF POD NEAR STRUT	025.3000000	004.4901888	007.7772350
	025.6500000	004.5080565	007.8081827
	026.1500000	004.5328385	007.8511063
	026.8700000	004.5670308	007.9103293
	027.8900000	004.6125688	007.9892033
	029.3200000	004.6709889	008.0903898
	031.3300000	004.7431782	008.2154255
	034.1300000	004.8262660	008.3593377
	038.0000000	004.9116732	008.5072674
	042.0000000	004.9685366	008.6057576
	046.0000000	004.9964966	008.6541857
	050.0000000	004.9964459	008.6540979
	054.0000000	004.9671792	008.6034065
	058.0000000	004.9055322	008.4966308
	062.0000000	004.8065688	008.3252212
	066.0000000	004.6638044	008.0779459
	070.0000000	004.4694461	007.7413075
	073.0000000	004.2845164	007.4209999
	075.0000000	004.1403407	007.1712804
	025.0000000	002.5567314	008.5760514
	025.0700000	002.6481748	008.5559700
	025.3000000	002.7500891	008.5489292
	025.6500000	002.8467084	008.5549133
	026.1500000	002.9493932	008.5724895
	026.8700000	003.0662163	008.6040338
	027.8900000	003.1998724	008.6523973
	029.3200000	003.3512592	008.7201838
	031.3300000	003.5192219	008.8094287
	034.1300000	003.6940691	008.9176917
	038.0000000	003.8567144	009.0345939
	042.0000000	003.9565937	009.1154149
	046.0000000	004.0056022	009.1550565
	050.0000000	004.0121755	009.1520671
	054.0000000	003.9754393	009.1042495
	058.0000000	003.8861994	009.0085757
	062.0000000	003.7285507	008.8606051
	066.0000000	003.4816709	008.6534532
	070.0000000	003.1207402	008.3764415
	073.0000000	002.7550289	008.1140703
	075.0000000	002.3836662	007.9301842
	025.0000000	000.4997399	008.9350877
	025.0700000	000.6864794	008.9300725
	025.3000000	000.8864286	008.9365220
	025.6500000	001.0691783	008.9524939
	026.1500000	001.2572945	008.9780681
	026.8700000	001.4649355	009.0158219
	027.8900000	001.6956001	009.0679712
	029.3200000	001.9494179	009.1363184
	031.3300000	002.2228832	009.2222420
	034.1300000	002.4986879	009.3235149
	038.0000000	002.7461612	009.4316877
	042.0000000	002.8932115	009.5065635
	046.0000000	002.9652600	009.5429106
	050.0000000	002.9790171	009.5385188
	054.0000000	002.9339763	009.4912201
	058.0000000	002.8143359	009.3987496
	062.0000000	002.5920797	009.2570803
	066.0000000	002.2303615	009.0570289
	070.0000000	001.6852358	008.7785974
	073.0000000	001.1197471	008.4955570

	X	Y	Z
	075.0000000	000.4996962	008.2655905
	025.0000000	000.0000000	008.9490520
	025.0700000	000.1871395	008.9544642
	025.3000000	000.3877534	008.9720025
	025.6500000	000.5713172	008.9979935
	026.1500000	000.7604658	009.0337250
	026.8700000	000.9694601	009.0824682
	027.8900000	001.2018688	009.1465114
	029.3200000	001.4578667	009.2275224
	031.3300000	001.7339418	009.3265430
	034.1300000	002.0125953	009.4403831
	038.0000000	002.2627473	009.5591898
	042.0000000	002.4114135	009.6400471
	046.0000000	002.4842683	009.6792728
	050.0000000	002.4982230	009.6755757
	054.0000000	002.4527661	009.6268071
	058.0000000	002.3319022	009.5299115
	062.0000000	002.1073108	009.3793206
	066.0000000	001.7418944	009.1635194
	070.0000000	001.1918220	008.8590831
	073.0000000	000.6224102	008.5463985
	075.0000000	000.0000000	008.2806814
STRUT	025.0000000	000.0000000	008.9490520
	025.0700000	000.1871395	008.9544642
	025.3000000	000.3877534	008.9720025
	025.6500000	000.5713172	008.9979935
	026.1500000	000.7604658	009.0337250
	026.8700000	000.9694601	009.0824682
	027.8900000	001.2018688	009.1465114
	029.3200000	001.4578667	009.2275224
	031.3300000	001.7339418	009.3265430
	034.1300000	002.0125953	009.4403831
	038.0000000	002.2627473	009.5591898
	042.0000000	002.4114135	009.6400471
	046.0000000	002.4842683	009.6792728
	050.0000000	002.4982230	009.6755757
	054.0000000	002.4527661	009.6268071
	058.0000000	002.3319022	009.5299115
	062.0000000	002.1073108	009.3793206
	066.0000000	001.7418944	009.1635194
	070.0000000	001.1918220	008.8590831
	073.0000000	000.6224102	008.5463985
	075.0000000	000.0000000	008.2806814
	025.0000000	000.0000000	009.4490520
	025.0700000	000.1871395	009.4544642
	025.3000000	000.3877534	009.4720025
	025.6500000	000.5713172	009.4979935
	026.1500000	000.7604658	009.5337250
	026.8700000	000.9694601	009.5824682
	027.8900000	001.2018688	009.6465114
	029.3200000	001.4578667	009.7275224
	031.3300000	001.7339418	009.8265430
	034.1300000	002.0125953	009.9403831
	038.0000000	002.2627473	010.0591898
	042.0000000	002.4114135	010.1400471
	046.0000000	002.4842683	010.1792728
	050.0000000	002.4982230	010.1755757
	054.0000000	002.4527661	010.1268071
	058.0000000	002.3319022	010.0299115
	062.0000000	002.1073108	009.8793206

	X	Y	Z
	066.0000000	001.7418944	009.6635194
	070.0000000	001.1918220	009.3590831
	073.0000000	000.6224102	009.0463985
	075.0000000	000.0000000	008.7806814
	025.0000000	000.0000000	011.0000000
	025.0700000	000.1871395	011.0000000
	025.3000000	000.3877534	011.0000000
	025.6500000	000.5713172	011.0000000
	026.1500000	000.7604658	011.0000000
	026.8700000	000.9694601	011.0000000
	027.8900000	001.2018688	011.0000000
	029.3200000	001.4578667	011.0000000
	031.3300000	001.7339418	011.0000000
	034.1300000	002.0125953	011.0000000
	038.0000000	002.2627473	011.0000000
	042.0000000	002.4114135	011.0000000
	046.0000000	002.4842683	011.0000000
	050.0000000	002.4982230	011.0000000
	054.0000000	002.4527661	011.0000000
	058.0000000	002.3319022	011.0000000
	062.0000000	002.1073108	011.0000000
	066.0000000	001.7418944	011.0000000
	070.0000000	001.1918220	011.0000000
	073.0000000	000.6224102	011.0000000
	075.0000000	000.0000000	011.0000000
	025.0000000	000.0000000	999.9999999
	025.0700000	000.1871395	999.9999999
	025.3000000	000.3877534	999.9999999
	025.6500000	000.5713172	999.9999999
	026.1500000	000.7604658	999.9999999
	026.8700000	000.9694601	999.9999999
	027.8900000	001.2018688	999.9999999
	029.3200000	001.4578667	999.9999999
	031.3300000	001.7339418	999.9999999
	034.1300000	002.0125953	999.9999999
	038.0000000	002.2627473	999.9999999
	042.0000000	002.4114135	999.9999999
	046.0000000	002.4842683	999.9999999
	050.0000000	002.4982230	999.9999999
	054.0000000	002.4527661	999.9999999
	058.0000000	002.3319022	999.9999999
	062.0000000	002.1073108	999.9999999
	066.0000000	001.7418944	999.9999999
	070.0000000	001.1918220	999.9999999
	073.0000000	000.6224102	999.9999999
	075.0000000	000.0000000	999.9999999
LOWER SURFACE OF FOIL	025.0000000	008.9490520	-000.0000000
	025.0700000	008.9544642	-000.1871395
	025.3000000	008.9720025	-000.3877534
	025.6500000	008.9979935	-000.5713172
	026.1500000	009.0337250	-000.7604658
	026.8700000	009.0824682	-000.9694601
	027.8900000	009.1465114	-001.2018688
	029.3200000	009.2275224	-001.4578667
	031.3300000	009.3265430	-001.7339418
	034.1300000	009.4403831	-002.0125953
	038.0000000	009.5591898	-002.2627473
	042.0000000	009.6400471	-002.4114135
	046.0000000	009.6792728	-002.4842683
	050.0000000	009.6755757	-002.4982230

TABLE 5 - CONTINUED

X	Y	Z
054.0000000	009.6268071	-002.4527661
058.0000000	009.5299115	-002.3319022
062.0000000	009.3793206	-002.1073108
066.0000000	009.1635194	-001.7418944
070.0000000	008.8590831	-001.1918220
073.0000000	008.5463985	-000.6224102
075.0000000	008.2806814	-000.0000000
025.0000000	009.4490520	-000.0000000
025.0700000	009.4544642	-000.1871395
025.3000000	009.4720025	-000.3877534
025.6500000	009.4979935	-000.5713172
026.1500000	009.5337250	-000.7604658
026.8700000	009.5824682	-000.9694601
027.8900000	009.6465114	-001.2018688
029.3200000	009.7275224	-001.4578667
031.3300000	009.8265430	-001.7339418
034.1300000	009.9403831	-002.0125953
038.0000000	010.0591898	-002.2627473
042.0000000	010.1400471	-002.4114135
046.0000000	010.1792728	-002.4842683
050.0000000	010.1755757	-002.4982230
054.0000000	010.1268071	-002.4527661
058.0000000	010.0299115	-002.3319022
062.0000000	009.8793206	-002.1073108
066.0000000	009.6635194	-001.7418944
070.0000000	009.3590831	-001.1918220
073.0000000	009.0463985	-000.6224102
075.0000000	008.7806814	-000.0000000
025.0000000	011.0000000	-000.0000000
025.0700000	011.0000000	-000.1871395
025.3000000	011.0000000	-000.3877534
025.6500000	011.0000000	-000.5713172
026.1500000	011.0000000	-000.7604658
026.8700000	011.0000000	-000.9694601
027.8900000	011.0000000	-001.2018688
029.3200000	011.0000000	-001.4578667
031.3300000	011.0000000	-001.7339418
034.1300000	011.0000000	-002.0125953
038.0000000	011.0000000	-002.2627473
042.0000000	011.0000000	-002.4114135
046.0000000	011.0000000	-002.4842683
050.0000000	011.0000000	-002.4982230
054.0000000	011.0000000	-002.4527661
058.0000000	011.0000000	-002.3319022
062.0000000	011.0000000	-002.1073108
066.0000000	011.0000000	-001.7418944
070.0000000	011.0000000	-001.1918220
073.0000000	011.0000000	-000.6224102
075.0000000	011.0000000	-000.0000000
025.0000000	999.9999999	-000.0000000
025.0700000	999.9999999	-000.1871395
025.3000000	999.9999999	-000.3877534
025.6500000	999.9999999	-000.5713172
026.1500000	999.9999999	-000.7604658
026.8700000	999.9999999	-000.9694601
027.8900000	999.9999999	-001.2018688
029.3200000	999.9999999	-001.4578667
031.3300000	999.9999999	-001.7339418
034.1300000	999.9999999	-002.0125953
038.0000000	999.9999999	-002.2627473

	X	Y	Z
	042.0000000	999.9999999	-002.4114135
	046.0000000	999.9999999	-002.4842683
	050.0000000	999.9999999	-002.4982230
	054.0000000	999.9999999	-002.4527661
	058.0000000	999.9999999	-002.3319022
	062.0000000	999.9999999	-002.1073108
	066.0000000	999.9999999	-001.7418944
	070.0000000	999.9999999	-001.1918220
	073.0000000	999.9999999	-000.6224102
	075.0000000	999.9999999	-000.0000000
UPPER	025.0000000	999.9999999	000.0000000
SURFACE	025.0700000	999.9999999	000.1871395
OF FOIL	025.3000000	999.9999999	000.3877534
	025.6500000	999.9999999	000.5713172
	026.1500000	999.9999999	000.7604658
	026.8700000	999.9999999	000.9694601
	027.8900000	999.9999999	001.2018688
	029.3200000	999.9999999	001.4578667
	031.3300000	999.9999999	001.7339418
	034.1300000	999.9999999	002.0125953
	038.0000000	999.9999999	002.2627473
	042.0000000	999.9999999	002.4114135
	046.0000000	999.9999999	002.4842683
	050.0000000	999.9999999	002.4982230
	054.0000000	999.9999999	002.4527661
	058.0000000	999.9999999	002.3319022
	062.0000000	999.9999999	002.1073108
	066.0000000	999.9999999	001.7418944
	070.0000000	999.9999999	001.1918220
	073.0000000	999.9999999	000.6224102
	075.0000000	999.9999999	000.0000000
	025.0000000	260.0000000	000.0000000
	025.0700000	260.0000000	000.1871395
	025.3000000	260.0000000	000.3877534
	025.6500000	260.0000000	000.5713172
	026.1500000	260.0000000	000.7604658
	026.8700000	260.0000000	000.9694601
	027.8900000	260.0000000	001.2018688
	029.3200000	260.0000000	001.4578667
	031.3300000	260.0000000	001.7339418
	034.1300000	260.0000000	002.0125953
	038.0000000	260.0000000	002.2627473
	042.0000000	260.0000000	002.4114135
	046.0000000	260.0000000	002.4842683
	050.0000000	260.0000000	002.4982230
	054.0000000	260.0000000	002.4527661
	058.0000000	260.0000000	002.3319022
	062.0000000	260.0000000	002.1073108
	066.0000000	260.0000000	001.7418944
	070.0000000	260.0000000	001.1918220
	073.0000000	260.0000000	000.6224102
	075.0000000	260.0000000	000.0000000
	025.0000000	140.0000000	000.0000000
	025.0700000	140.0000000	000.1871395
	025.3000000	140.0000000	000.3877534
	025.6500000	140.0000000	000.5713172
	026.1500000	140.0000000	000.7604658
	026.8700000	140.0000000	000.9694601
	027.8900000	140.0000000	001.2018688
	029.3200000	140.0000000	001.4578667

X	Y	Z
031.3300000	140.0000000	001.7339418
034.1300000	140.0000000	002.0125953
038.0000000	140.0000000	002.2627473
042.0000000	140.0000000	002.4114135
046.0000000	140.0000000	002.4842683
050.0000000	140.0000000	002.4982230
054.0000000	140.0000000	002.4527661
058.0000000	140.0000000	002.3319022
062.0000000	140.0000000	002.1073108
066.0000000	140.0000000	001.7418944
070.0000000	140.0000000	001.1918220
073.0000000	140.0000000	000.6224102
075.0000000	140.0000000	000.0000000
025.0000000	060.0000000	000.0000000
025.0700000	060.0000000	000.1871395
025.3000000	060.0000000	000.3877534
025.6500000	060.0000000	000.5713172
026.1500000	060.0000000	000.7604658
026.8700000	060.0000000	000.9694601
027.8900000	060.0000000	001.2018688
029.3200000	060.0000000	001.4578667
031.3300000	060.0000000	001.7339418
034.1300000	060.0000000	002.0125953
038.0000000	060.0000000	002.2627473
042.0000000	060.0000000	002.4114135
046.0000000	060.0000000	002.4842683
050.0000000	060.0000000	002.4982230
054.0000000	060.0000000	002.4527661
058.0000000	060.0000000	002.3319022
062.0000000	060.0000000	002.1073108
066.0000000	060.0000000	001.7418944
070.0000000	060.0000000	001.1918220
073.0000000	060.0000000	000.6224102
075.0000000	060.0000000	000.0000000
025.0000000	040.0000000	000.0000000
025.0700000	040.0000000	000.1871395
025.3000000	040.0000000	000.3877534
025.6500000	040.0000000	000.5713172
026.1500000	040.0000000	000.7604658
026.8700000	040.0000000	000.9694601
027.8900000	040.0000000	001.2018688
029.3200000	040.0000000	001.4578667
031.3300000	040.0000000	001.7339418
034.1300000	040.0000000	002.0125953
038.0000000	040.0000000	002.2627473
042.0000000	040.0000000	002.4114135
046.0000000	040.0000000	002.4842683
050.0000000	040.0000000	002.4982230
054.0000000	040.0000000	002.4527661
058.0000000	040.0000000	002.3319022
062.0000000	040.0000000	002.1073108
066.0000000	040.0000000	001.7418944
070.0000000	040.0000000	001.1918220
073.0000000	040.0000000	000.6224102
075.0000000	040.0000000	000.0000000
025.0000000	020.0000000	000.0000000
025.0700000	020.0000000	000.1871395
025.3000000	020.0000000	000.3877534
025.6500000	020.0000000	000.5713172
026.1500000	020.0000000	000.7604658

TABLE 5 - CONTINUED

UPPER SURFACE OF FOIL (CONT.)

X	Y	Z
026.8700000	020.0000000	000.9694601
027.8900000	020.0000000	001.2018688
029.3200000	020.0000000	001.4578667
031.3300000	020.0000000	001.7339418
034.1300000	020.0000000	002.0125953
038.0000000	020.0000000	002.2627473
042.0000000	020.0000000	002.4114135
046.0000000	020.0000000	002.4842683
050.0000000	020.0000000	002.4982230
054.0000000	020.0000000	002.4527661
058.0000000	020.0000000	002.3319022
062.0000000	020.0000000	002.1073108
066.0000000	020.0000000	001.7418944
070.0000000	020.0000000	001.1918220
073.0000000	020.0000000	000.6224102
075.0000000	020.0000000	000.0000000
025.0000000	011.0000000	000.0000000
025.0700000	011.0000000	000.1871395
025.3000000	011.0000000	000.3877534
025.6500000	011.0000000	000.5713172
026.1500000	011.0000000	000.7604658
026.8700000	011.0000000	000.9694601
027.8900000	011.0000000	001.2018688
029.3200000	011.0000000	001.4578667
031.3300000	011.0000000	001.7339418
034.1300000	011.0000000	002.0125953
038.0000000	011.0000000	002.2627473
042.0000000	011.0000000	002.4114135
046.0000000	011.0000000	002.4842683
050.0000000	011.0000000	002.4982230
054.0000000	011.0000000	002.4527661
058.0000000	011.0000000	002.3319022
062.0000000	011.0000000	002.1073108
066.0000000	011.0000000	001.7418944
070.0000000	011.0000000	001.1918220
073.0000000	011.0000000	000.6224102
075.0000000	011.0000000	000.0000000
025.0000000	009.1490519	000.0000000
025.0700000	009.1544641	000.1871395
025.3000000	009.1720024	000.3877534
025.6500000	009.1979934	000.5713172
026.1500000	009.2337250	000.7604658
026.8700000	009.2824681	000.9694601
027.8900000	009.3465114	001.2018688
029.3200000	009.4275223	001.4578667
031.3300000	009.5265429	001.7339418
034.1300000	009.6403830	002.0125953
038.0000000	009.7591897	002.2627473
042.0000000	009.8400470	002.4114135
046.0000000	009.8792727	002.4842683
050.0000000	009.8755757	002.4982230
054.0000000	009.8268070	002.4527661
058.0000000	009.7299114	002.3319022
062.0000000	009.5793205	002.1073108
066.0000000	009.3635193	001.7418944
070.0000000	009.0590830	001.1918220
073.0000000	008.7463984	000.6224102
075.0000000	008.4806813	000.0000000
025.0000000	008.9490520	000.0000000
025.0700000	008.9544642	000.1871395
025.3000000	008.9720025	000.3877534
025.6500000	008.9979935	000.5713172
026.1500000	009.0337250	000.7604658
026.8700000	009.0824682	000.9694601
027.8900000	009.1465114	001.2018688
029.3200000	009.2275224	001.4578667
031.3300000	009.3265430	001.7339418
034.1300000	009.4403831	002.0125953
038.0000000	009.5591898	002.2627473
042.0000000	009.6400471	002.4114135
046.0000000	009.6792728	002.4842683
050.0000000	009.6755757	002.4982230
054.0000000	009.6268071	002.4527661
058.0000000	009.5299115	002.3319022
062.0000000	009.3793206	002.1073108
066.0000000	009.1635194	001.7418944
070.0000000	008.8590831	001.1918220
073.0000000	008.5463985	000.6224102
075.0000000	008.2806814	000.0000000

INITIAL DISTRIBUTION

Copies		
27	CHBUSHIPS	
	2	Tech Lib (Code 210-L)
	1	Lab Mgt Div (Code 320)
	12	Prelim Des (Code 420)
	2	Hull Des (Code 440)
	2	Sci & Res (Code 442)
	4	Boats & Small Craft (Code 449)
	1	Ship Silencing Br (Code 345)
	1	Hull Mach & Arr Br (Code 632)
	1	Mine, Serv & Patrol Br (Code 526)
	1	Ships Research Br (Code 341B)
2	COMDT, U. S. Coast Guard	
2	CO, U. S. Army Transportation Research Command, Fort Eustis	
	1	Attention Tech Intelligence Br
	1	Attention Marine Transport Div
4	DIR, Davidson Lab, SIT, Hoboken	
2	ADMIN, Webb Inst of Naval Arch, Glen Cove	
	1	Attention Prof. Thomas M. Curran
	1	Attention Library
2	Head, Dept of NAME, MIT, Cambridge	
2	Head, Dept of NAME, Univ of Michigan, Ann Arbor	
1	AVCO Corporation, Wilmington	
		Attention Capt. F. X. Forest
1	DIR, Hudson Lab, Dobbs Ferry	
1	Sparkman and Stephans Inc., New York	
		Attention Mr. G. Gilbert Wyland
1	Franklin Systems, Inc., West Palm Beach	
		Attention Mr. D. J. W. McCarty
2	Chris-Craft Corp., Pompano Beach	
		Attention Mr. E. L. Eckfield
2	Gibbs and Cox, Inc.	
1	Republic Aviation Corp., Hydrospace Div., Farmingdale	
1	Owens Yacht Div., Brunswick Corp.	
		Attention Mr. David D. Beach
1	United Aircraft Corporate Systems Center, Farmington, Conn.	
		Attention Mr. Henry A. Arnold
1	Mr. J. G. Koelbel, Jr., Massapequa, N. Y.	
1	Mr. Philip L. Rhodes, New York	
20	DDC	
2	Chief, ONR (Code 438)	
2	Chief, BUWEPS	
	1	Attention Code RAAD-334
	1	Attention Code RRSY-1
1	Langley Aeronautical Lab, NASA	
1	CNO	
		Attention LCDR, W. Norris (OP-725)

1 Scientific and Technical Information Facility
  Attention NASA Representative (SAK/DL-504), Bethesda
1 Oceanics, Inc.
  Attention Dr. Paul Kaplan
1 Stanford University
  Attention Head, Civil Engineering
1 Boeing Airplane Company, Aero-Space Div., Marine Systems Group, Seattle
1 CIT, Hydrodynamics Laboratory
2 Hydronautics, Inc.
1 Univ of Minnesota, St. Anthony Falls Hydraulic Lab., Minneapolis
1 TRG
1 Aerojet General Corp., Azusa
  Attention Mr. J. Levy
1 Lockheed Aircraft Corp., Hydrodynamic Group, Sunnyvale
  Attention Mr. R. Waid
1 Grumman Aircraft Engineering Corp., Marine Engineering Section, Bethpag
2 DIR, USNRL (Code 2027)
1 Commander, Planning Dept., Philadelphia Naval Shipyard, U. S. Naval Base, Philadelphia 12
1 Superintendent, USNAVPGSCOL, Monterey
1 Superintendent, U. S. Naval Academy, Annapolis
  Attention Library
2 MARAD
  1 Attention Division of Ship Design
  1 Attention Division of Research
1 CO&D, USNMDL, Panama City
1 CO, MIT
  Attention NROTC and Naval Administrative Unit
1 NASA, Washington
  Attention Mr. J. B. Parkinson
1 DIR, National Science Foundation
  Attention Engineering Sciences Division
3 DIR, National Bureau of Standards
  1 Attention Dr. G. B. Schubauer
  1 Attention Dr. G. H. Keulegan
  1 Attention Dr. J. M. Franklin
1 Office of Technical Services, Dept of Commerce, Washington
3 CIT, Pasadena
  1 Attention Prof. M. S. Plesset
  1 Attention Prof. T. Y. Wu
  1 Prof. A. J. Acosta
2 University of California, Berkeley, Dept of Engineering
  1 Attention Dr. A. Powell
  1 Attention Prof. R. Paulling
3 University of Iowa, Iowa City
  1 Attention Dr. H. Rouse
  1 Attention Dr. L. Landweber
  1 Attention Inst of Hydraulic Research

1 MIT, Dept of NAME
Attention Prof. A. T. Ippen

1 Executive Director, Air Force Office of Scientific Research, Washington
Attention Mechanics Branch

1 NPL, Teddington, Middlesex, England, Superintendent of Ship Division
Attention Dr. A. Silverleaf

1 Dr. S. F. Hoerner, 148 Busteed Drive, Midland Park, New Jersey

1 Electric Boat Division, General Dynamics Corp., Groton
Attention Mr. Robert McCandliss

1 Lockheed Aircraft Corp., Missiles and Space Division, Palo Alto,
Attention R. W. Kermeen

2 Convair, Division of General Dynamics, San Diego
1 Attention Mr. R. H. Oversmith
1 Attention Mr. H. T. Brooke

1 Baker Manufacturing Company, Evansville, Wisconsin
Attention Mr. J. G. Baker

1 Lockheed Aircraft Corp., California Div., Hydrodynamics Res., Burbank, California
Attention Mr. Bill East

2 Stanford University, Dept of Civil Engineering, Stanford, Calif.
1 Attention Dr. Byrne Perry
1 Attention Dr. E. Y. Hsu

1 Radio Corp of America, Hydrofoil Projects, Burlington, Mass.
Attention Mr. David Wellinger

1 FMC, San Jose
Attention Mr. G. Tedrew

5 Douglas Aircraft Co, Aircraft Division, Long Beach, Calif.
Attention Mr. John L. Hess

1 Cornell Univ, Graduate School of Aero Engr., Ithaca, N. Y.
Attention Prof. W. R. Sears

Unclassified

Security Classification

DOCUMENT CONTROL DATA - R&D

(Security classification of title, body of abstract and indexing annotation must be entered when the overall report is classified)

1. ORIGINATING ACTIVITY *(Corporate author)*	2a. REPORT SECURITY CLASSIFICATION
David Taylor Model Basin Washington, D. C. 20007	Unclassified
	2b. GROUP

3. REPORT TITLE

Some Theoretical and Experimental Results on Pressure Interaction of Hydrofoil Boat Components

4. DESCRIPTIVE NOTES *(Type of report and inclusive dates)*

Final

5. AUTHOR(S) *(Last name, first name, initial)*

Moore, Wilburn L.

6. REPORT DATE	7a. TOTAL NO. OF PAGES	7b. NO. OF REFS
November 1965	47	15

8a. CONTRACT OR GRANT NO.	9a. ORIGINATOR'S REPORT NUMBER(S)
b. Sub-PROJECT NO. SS-600-000	2131
c. Task 1703	9b. OTHER REPORT NO(S) *(Any other numbers that may be assigned this report)*
d	

10. AVAILABILITY/LIMITATION NOTICES

This document is subject to special export controls and each transmittal to foreign nationals may be made only with prior approval of the Bureau of Ships.

11. SUPPLEMENTARY NOTES	12. SPONSORING MILITARY ACTIVITY
	Bureau of Ships

13. ABSTRACT

The Douglas Neumann program for non-lifting three-dimensional fluid flow is used to calculate the potential flow pressure distribution for some hydrofoil boat components in various combinations. The calculated results are compared with pressure measurements on crossed non-lifting foils, and on a lifting foil of large span in conjunction with a pod. The calculated results were corrected for lift in the latter case. These comparisons indicate that the Douglas program can be usefully applied to the hydrofoil-boat problems.

Pressure calculations are presented for non-lifting strut-foil, pod-foil and strut-pod-foil configurations. These results show that the effect of a strut on the pressure distribution of a pod-foil is appreciable, and that a pod can be used to increase the cavitation-inception speed of a strut-foil.

A discussion of how to select input points for the Douglas program for intersecting bodies is also presented.

DD FORM 1 JAN 64 1473

Unclassified

Security Classification

14. KEY WORDS	LINK A ROLE	LINK A WT	LINK B ROLE	LINK B WT	LINK C ROLE	LINK C WT
Cavitation, hydrofoils						
Hydrofoils, cavitation						
Hydrofoils, pressure calculation						
Hydrofoils, pressure measurements						
Pressure measurements						
Pressure interference						
Pressure interaction						
Interference, pressure						
Hydrofoil boat, struts						
Hydrofoil boat, foils						
Hydrofoil boat, pods						
Hydrofoil boat, interference effects						
Neumann problem						
Potential flow						
Goethert transformation						
Douglas Neumann program						
Airfoil interference						
Airfoils, compressibility						
Airfoils, subsonic flow						
Hydrodynamics, three-dimensional flow						
Aerodynamics, three-dimensional flow						
Three-dimensional fluid flow						

INSTRUCTIONS

1. ORIGINATING ACTIVITY: Enter the name and address of the contractor, subcontractor, grantee, Department of Defense activity or other organization *(corporate author)* issuing the report.

2*a*. REPORT SECURITY CLASSIFICATION: Enter the overall security classification of the report. Indicate whether "Restricted Data" is included. Marking is to be in accordance with appropriate security regulations.

2*b*. GROUP: Automatic downgrading is specified in DoD Directive 5200.10 and Armed Forces Industrial Manual. Enter the group number. Also, when applicable, show that optional markings have been used for Group 3 and Group 4 as authorized.

3. REPORT TITLE: Enter the complete report title in all capital letters. Titles in all cases should be unclassified. If a meaningful title cannot be selected without classification, show title classification in all capitals in parenthesis immediately following the title.

4. DESCRIPTIVE NOTES: If appropriate, enter the type of report, e.g., interim, progress, summary, annual, or final. Give the inclusive dates when a specific reporting period is covered.

5. AUTHOR(S): Enter the name(s) of author(s) as shown on or in the report. Enter last name, first name, middle initial. If military, show rank and branch of service. The name of the principal author is an absolute minimum requirement.

6. REPORT DATE: Enter the date of the report as day, month, year; or month, year. If more than one date appears on the report, use date of publication.

7*a*. TOTAL NUMBER OF PAGES: The total page count should follow normal pagination procedures, i.e., enter the number of pages containing information.

7*b*. NUMBER OF REFERENCES: Enter the total number of references cited in the report.

8*a*. CONTRACT OR GRANT NUMBER: If appropriate, enter the applicable number of the contract or grant under which the report was written.

8*b*, 8*c*, & 8*d*. PROJECT NUMBER: Enter the appropriate military department identification, such as project number, subproject number, system numbers, task number, etc.

9*a*. ORIGINATOR'S REPORT NUMBER(S): Enter the official report number by which the document will be identified and controlled by the originating activity. This number must be unique to this report.

9*b*. OTHER REPORT NUMBER(S): If the report has been assigned any other report numbers *(either by the originator or by the sponsor)*, also enter this number(s).

10. AVAILABILITY/LIMITATION NOTICES: Enter any limitations on further dissemination of the report, other than those imposed by security classification, using standard statements such as:

(1) "Qualified requesters may obtain copies of this report from DDC."

(2) "Foreign announcement and dissemination of this report by DDC is not authorized."

(3) "U. S. Government agencies may obtain copies of this report directly from DDC. Other qualified DDC users shall request through
____________________________."

(4) "U. S. military agencies may obtain copies of this report directly from DDC. Other qualified users shall request through
____________________________."

(5) "All distribution of this report is controlled. Qualified DDC users shall request through
____________________________."

If the report has been furnished to the Office of Technical Services, Department of Commerce, for sale to the public, indicate this fact and enter the price, if known.

11. SUPPLEMENTARY NOTES: Use for additional explanatory notes.

12. SPONSORING MILITARY ACTIVITY: Enter the name of the departmental project office or laboratory sponsoring *(paying for)* the research and development. Include address.

13. ABSTRACT: Enter an abstract giving a brief and factual summary of the document indicative of the report, even though it may also appear elsewhere in the body of the technical report. If additional space is required, a continuation sheet shall be attached.

It is highly desirable that the abstract of classified reports be unclassified. Each paragraph of the abstract shall end with an indication of the military security classification of the information in the paragraph, represented as *(TS)*, *(S)*, *(C)*, or *(U)*.

There is no limitation on the length of the abstract. However, the suggested length is from 150 to 225 words.

14. KEY WORDS: Key words are technically meaningful terms or short phrases that characterize a report and may be used as index entries for cataloging the report. Key words must be selected so that no security classification is required. Identifiers, such as equipment model designation, trade name, military project code name, geographic location, may be used as key words but will be followed by an indication of technical context. The assignment of links, roles, and weights is optional.